Early detection of peritonitis using non-invasive laser scattering

Master's thesis
by
Edward Birch-Iensen and Mikael Karlsson

Lund Reports on Atom Physics, LRAP-359
Lund, June 2006

Tidig detektion av peritonit med användande av laserljusspridning

Peritonealdialys (PD) är en behandlingsmetod för patienter som lider av njursvikt. I PD filtreras slaggprodukter och överflödsvätska från blodet genom bukhinnan till en dialysvätska som förts in i bukhålan. Dialysvätskan förs in via en kateter i bukväggen som skapar en förbindelse mellan utsidan av buken och bukhålan (**Figur 1**).

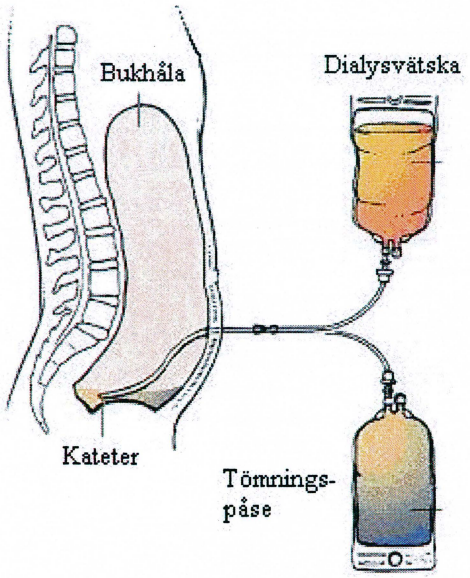

Figur 1. Peritonealdialys.

När patienten kopplar en påse med dialysvätska till katetern finns det risk för kontamination som kan leda till en inflammation av bukhinnan (peritonit). Detta livshotande tillstånd är den största orsaken till varför patienter måste lämna PD-behandling och drabbar peritonealdialyspatienter i genomsnitt en gång var 24:e månad. Peritoniten kan skada bukhinnan permanent och påverka dess förmåga att fungera som ett dialysfilter. Detta innebär att patienten måste övergå till hemodialys (bloddialys) vilket oftast utförs på klinik och minskar patientens frihet.

När en patient får peritonit är det viktigt att påbörja behandlingen så fort som möjligt. I detta examensarbete har en ny optisk metod för tidig upptäckt av peritonit testats. Ett av de viktigaste tecknen på att en patient kan ha en peritonit är att den uttömda vätskan blir grumlig. Denna grumlighet beror på att antalet vita blodkroppar ökar och en prototyp som utvecklats på Gambro, kallad Gambro Peritonit Detektor (GPD), mäter denna grumlighet med hjälp av spridning av laserljus.

En cellkoncentration större än 100 celler/µl är vanligtvis en indikation på peritonit. Genom att fokusera en laserstråle genom slangen med det utrinnande dialysatet kunde celler detekteras då de passerade laserstrålen. Vid denna passage reflekterades laserljus till en ljusdetektor. Analys av signalen från ljusdetektorn gav ett samband mellan signal och cellkoncentration.

Resultaten från GPD:n verkade lovande för att i framtiden kunna följa en ökning i cellkoncentration i dialysat och varna patienten om en annalkande peritonit (**Figur 2**).

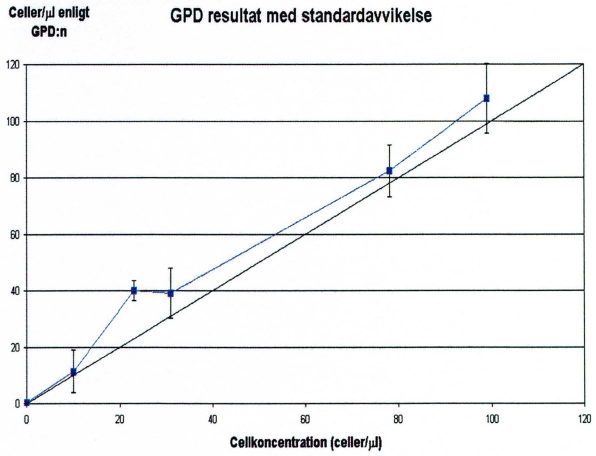

Figur 2. Resultat från GPD:n med standardavvikelse från mätningar på dialysvätska med 0-, 10-, 23-, 31-, 78-, och 99 celler/µl.

Med GPD:n installerad hos varje patient som går på peritonealdialys, borde antalet allvarliga konsekvenser av peritonit kunna minskas drastiskt.

Abstract

Peritoneal dialysis (PD) is one out of three treatment options available when suffering from end stage renal disease (ESRD). The others being kidney transplant and haemodialysis (HD). The biggest Achilles heel for PD treatment today is peritonitis. It's the main reason for patients leaving PD. An episode of peritonitis is not only costly and unpleasant for the patient but could also have fatal outcome. Therefore the opportunity to make an early diagnosis of peritonitis is a question of life and death for PD patients. This diploma work explores the opportunity to analyze the effluent dialysate through non-invasive techniques and thereby obtaining early signs of an oncoming episode of peritonitis. The GPD (Gambro Peritonitis Detector), a prototype built by Gambro, measuring light scattering through dialysate was tested and evaluated. Other possible methods were also explored. The light scattering measurements were made through the tube sets used in Gambro's automated peritoneal dialysis (APD) machine Serena^{TM}. The intention of the light scattering measurements was to detect elevated cell counts in the dialysate, which is an indication of peritonitis. The results from the GPD showed good consistency with conventional cell counters that were used as a reference, both with L929 cells cultivated in the lab as well as with dialysate obtained from PD clinics. The GPD shows great promise for a cheap, automated watch on PD patients concerning early indications of peritonitis.

Table of contents

Abbreviations and acronyms

APD – Automated Peritoneal Dialysis
CAPD – Continuous Ambulatory Peritoneal Dialysis
CCD – Charged-Coupled Device
DAQ – Data acquisition
HD – Haemodialysis
PD – Peritoneal dialysis
PVC – Polyvinyl chloride
GPD – Gambro Peritonitis Detector
WBC – White blood cell

1. Introduction

1.1. Peritoneal dialysis (PD)

Dialysis or transplantation is needed to treat the life threatening condition resulting from kidney failure. There are two types of dialysis, haemodialysis (HD) and peritoneal dialysis (PD). In HD blood is extracted from the patient's body and filtered through a machine. The machine removes waste products and excess fluid from the blood through a membrane filter before the treated blood is returned to the patient. PD works through the same principle but instead of using manufactured filters, the peritoneal membrane of the patient is used as a filter [1]. The waste products and excess fluid is filtered from the blood through the peritoneal membrane into a fluid that has been introduced into the peritoneal cavity (see Figure 1).

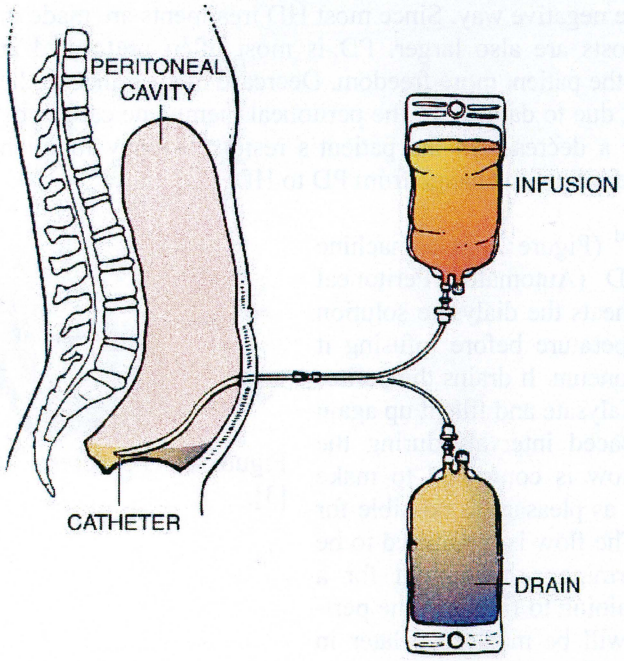

Figure 1. Peritoneal dialysis [2].

There are about 150 000 patients worldwide currently undergoing PD treatment. In peritoneal dialysis the peritoneal membrane is used as a semi-permeable filter. A catheter is surgically implanted in the abdomen making a connection from outside the patient to the peritoneal cavity. The peritoneal cavity is flooded with a glucose solution. The solution creates an osmotic drag removing fluid from the patient into the fluid in the peritoneal cavity. At regular intervals the fluid is exchanged. There are mainly two types of PD,

manual and automated. They work according the same principle. Filling the peritoneal cavity with solution enables the waste products and excess fluid in the blood to pass through the peritoneal membrane to the glucose solution. The time the fluid rests in the abdomen is called dwell time. Different types of PD use different schedules for dwell times and exchanges. The main advantage in PD in comparison to HD is that the PD treatment keeps the level of toxins more constant. This is due to more frequent and evenly spaced treatments instead of the few set appointments at the hospital where level of toxins in the body is, through HD, decreased under a shorter period of time. The HD treatment can clean a larger amount of blood per time unit than the PD treatment can i.e. it has a higher clearance. This treatment could therefore be done in a shorter period of time. The HD treatment changes the levels of toxins more drastically in the patient than when the patient is treated with PD. This means that the patient may spend a longer time accumulating waste products in the body before visiting the hospital and in a matter of hours reducing the high concentration of waste products drastically. Exposing the body for a high variation in concentrations of waste products could affect the residual kidney function in a more negative way. Since most HD treatments are made in clinics the costs are also larger. PD is most often preformed at home giving the patient more freedom. Decrease of clearance in the PD treatment due to damage of the peritoneal membrane caused by peritonitis or a decrease in the patient's residual kidney function may force the patient to change from PD to HD.

The Serena™ (Figure 2) is a machine used in APD (Automated Peritoneal Dialysis). It heats the dialysate solution to body temperature before infusing it into the peritoneum. It drains the peritoneum from dialysate and fills it up again in evenly spaced intervals during the night. The flow is controlled to make the treatment as pleasant as possible for the patient. The flow is monitored to be able to determine a breakpoint for a shift from draining to filling of the peritoneum. As will be mentioned later in this report the flow is an important parameter for determine the concentration of cells in the effluent dialysate.

Figure 2. The Serena™ [3].

1.1.1. Peritonitis

Peritonitis is the main reason for failure in PD treatment (Figure 3). Peritonitis is an inflammation of the peritoneal membrane. The prognosis for untreated peritonitis is very poor. The inflammation of the peritoneal membrane may give permanent damage to the membrane and affect its ability to act as a dialysis filter. If the func-

tion of the membrane is affected by the inflammation it may force the patient to leave the PD treatment.

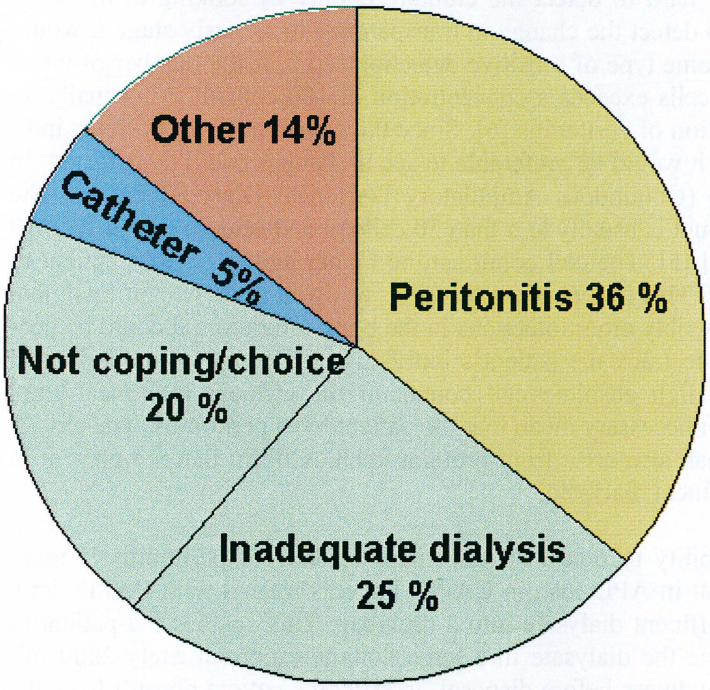

Figure 3. Reasons for transfer from long-term PD to HD [4].

The costs to treat an episode of peritonitis are substantial and in 1-6% of the cases the outcome is fatal in spite of treatment [1]. Therefore it's important that as soon as possible detect and begin treatment of peritonitis. For PD patients a common source of peritonitis is touch contamination. Patients accidentally touch the catheter and thereby make it possible for bacteria to gain entry. There is also the possibility of bacteria residing on the skin to gain entry through the peritoneal catheter tract. Bacteria of intestinal origin may enter the peritoneal cavity by migrating through the bowel wall and thereby causing peritonitis. To diagnose peritonitis at least two out of the three criteria (a-c) should be present [5].

a. Cloudy peritoneal fluid
b. Symptoms of peritonitis
c. Demonstration of bacteria in the peritoneal effluent by Gram's stain or culture.

The effluent fluid from the patient's peritoneal cavity is often observed for cloudiness as a first sign of peritonitis. The sudden appearance of cloudy peritoneal fluid is sufficient to start further investigation of the patient's condition. Symptoms in order of occurrence are abdominal pain, nausea and vomiting, feverish sensation, chills, constipation or diarrhea [5]. Common signs are besides cloudy peritoneal fluid, abdominal tenderness and increased body temperature. The cloudy peritoneal fluid is partly a consequence of

the increased number of white blood cells in the dialysate. At an early stage of peritonitis when the cell concentration still is low it can be hard to detect the cloudiness only by looking at it. To be able to detect the change in transparency in an early stage it would need some type of sensitive detection setup. If the number of white blood cells exceeds a concentration of 100 cells/µl it is usually an indication of peritonitis [6]. Since the concentration of cells is individual it would be preferable to see if changes could be detected. In CAPD (Continuous Ambulatory Peritoneal Dialysis) patients the cell count is usually less than 50 cells/µl and seldom higher than 10 cells/µl [5]. The cell count can be higher and vary from patient to patient. This is dependent on things as dwell time, way of treatment and possibly other infections in the body. Therefore it could be necessary to track the patient's individual cell count in the peritoneal fluid. High absolute cell counts in the effluent peritoneal fluid doesn't necessary mean that the patient have peritonitis. The cloudy fluid can also arise from proteins such as fibrin that are present in the effluent dialysate.

The ability to detect an oncoming episode of peritonitis is more difficult in APD than in CAPD. Patients treated with CAPD drain their effluent dialysate into a drainbag. This enables the patient to examine the dialysate in a large volume (approximately 2000 ml) for cloudiness before disposal. In APD the patient doesn't have the ability to examine the effluent dialysate in the same way. When a patient is treated with APD the effluent dialysate is directly drained into sewers and therefore the patient lacks the ability to examine it in a large volume. Many APD treatments are performed during the night while the patient is asleep which further reduces the possibility of detecting an increase of cloudiness in the effluent dialysate. The first step towards implementing an automated control of cell concentrations should be within APD where examination of the effluent dialysate is more difficult for the patient.
Peritonitis is often treated with intra-peritoneal antibiotics. It's not uncommon for a patient to have a relapsing peritonitis i.e. another episode of peritonitis caused by the same pathogen. On average there are about 0.5 episodes/patient year, which means that there is one new patient affected by this condition every 7:th minute worldwide.

1.1.1.1. How early can peritonitis be detected?

Bacteria introduced into the body give rise to an increased concentration of white blood cells in the affected area. This starts the inflammatory reaction of the body. As in any infection this is what happens in the case of peritonitis. The ability of catching peritonitis at an early stage is indirectly supported by a study made on how the ultrafiltration in PD patients is affected before, during and after episodes of peritonitis. Ultrafiltration is the transport of a fluid through a membrane caused by a pressure gradient. In the case of PD the

fluid is water, the membrane is the peritoneal membrane and the osmotic pressure gradient is caused by the dialysis fluid containing a higher concentration of glucose [7]. The osmotic forced ultrafiltration is known to decrease before, during and after episodes of peritonitis. Studies made by Albrektsen et al [8] shows that ultrafiltration decreases significantly up till 2 days before the diagnosis of peritonitis was made.

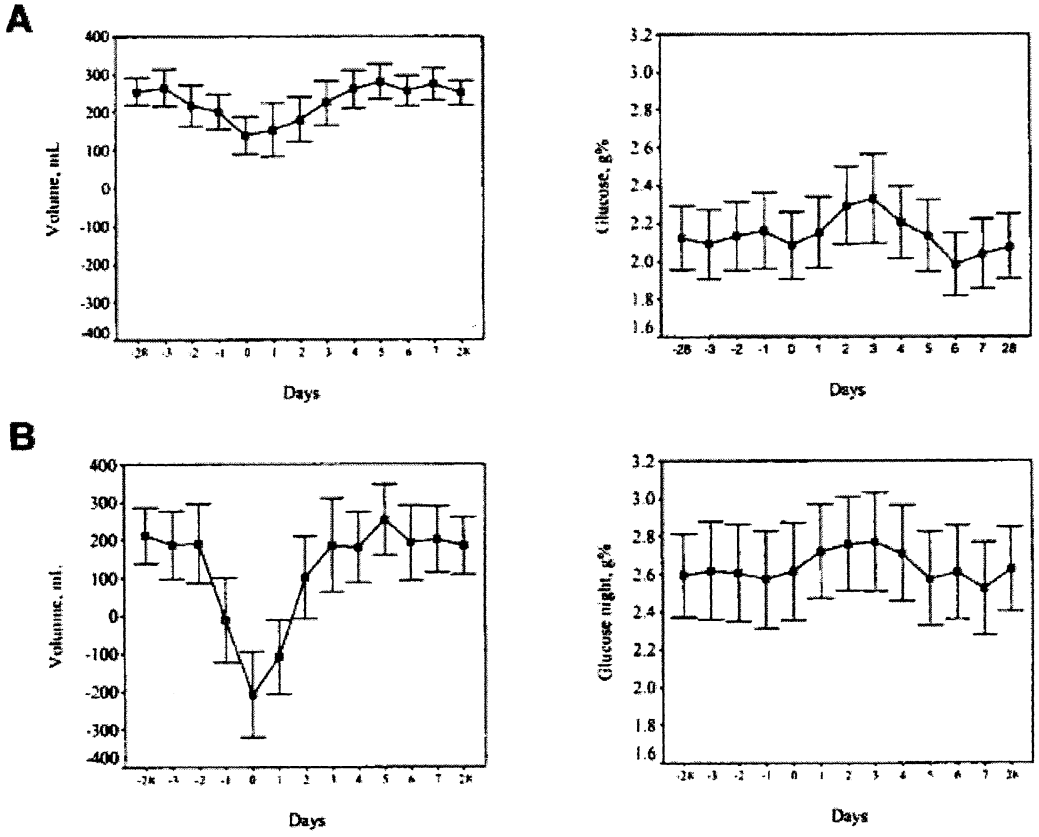

Figure 4. Mean drained ultrafiltration volume and glucose concentration in dialysis fluid the days around the diagnosis of peritonitis for (A) day and (B) night exchanges, with 95% confidence intervals, for 64 episodes of peritonitis. Day 0 refers to the day of diagnosis, and -28 and 28 refer to mean values for the months before and after diagnosis, respectively. Significant changes in ultrafiltration volumes relative to the month before (-28) appeared 2 and 1 day before the diagnosis of peritonitis for the day and night exchanges, respectively. Glucose concentrations did not change significantly relative to the month before. (Figure and caption from Albrektsen et al [8]).

The ultrafiltration is something that is affected by the inflammatory response of the body and should therefore in a way be related to the concentration of white blood cells. Therefore the ambition to catch the onset of an episode of peritonitis as much as two days before it truly manifests itself to the patient shouldn't be that far fetched.

1.1.2. Available methods for early indication of peritonitis

Today there is a scarce selection for simple and cheap automated methods to indicate peritonitis. Apart from the patient's ability to recognize symptoms or warnings of a future episode of peritonitis there are different test strips available for instant analysis. One example is the Serim™ Periscreen™ test strips. These test strips are recognized as a good tool in detecting peritonitis [9]. The strips detects the elevated leukocyte count (>100 cells/µl) mainly due to neutrophils (>50%) [10]. The procedure of making an analysis with these strips requires the possibility of direct contact to the peritoneal dialysate effluent. The indicator pad on the strip is immersed into the peritoneal dialysate effluent and quickly retracted. Then a timer should be started and four minutes later the color on the indicator pad can be compared with the color chart on the bottle. The chart shows four grades; negative, trace, small and large. The current price for such strips is about 25 € for a bottle containing 10 strips.

1.2. Light scattering

The way light scatters is dependent on the wavelength of the light as well as the size and optical properties of the particle it interacts with. There are different theories that describe the way light scatters. The geometrical description of light is applicable for particles that are much larger than the wavelength of the scattered light. It's a description that uses ray tracing and refraction laws to describe in which way the light scatters.

Particles that are about the same order of magnitude as the wavelength of light can cause Mie scattering. It's a theory that can explain why clouds built up by small droplets of water are white even though water is optically transparent. If particles are small compared to the wavelength of the light the scattering can be described with Rayleigh theory. It's a model that can explain why the sky is blue. There are many experiments made on how accurate the different models are under certain circumstances [11].

The laser used in experiments in this diploma work has a wavelength of approximately 635 nm. The white blood cells are about 7 - 20 µm in diameter. The effluent dialysate coming from the patient may contain other particles and cells in different sizes. Some examples are proteins, bacteria, white and red blood cells and air bubbles. These different objects vary in size and optical properties and could therefore be applicable to different light scattering theories [12,13].

The effluent fluid from the patient flows inside the PVC tube. The PVC tube itself may contribute additional scattering phenomenon.

Examination of cells regarding their concentration and size distribution can be done by means of light scattering. There are many different setups used for light scattering measurements within biology and medicine.

The need to determine concentrations of white blood cells is not unique for analysis of effluent dialysate. White blood cell concentration is a parameter often used in medicine and new ways of analyzing are continuously explored [14]. Linear relationships between scattered light intensity and cell concentration of both red and white blood cells have been established for stationary suspensions [15].

For laboratory use there are a variety of different instruments available for measuring concentrations and sizes of bacteria and cells. Light scattering can also be used for determining the aggregation of cells [16].

Urine analysers can determine the amount of bacteria, white blood cells and red blood cells. For detecting white blood cells urine analyser today have working range up to 4500 WBC/µl and a detection limit of about 3.2 WBC/µl [17]. The urine analysers are costly and require that a sample is put into a cuvette and often stained with some type of fluorescent dye.

1.3. Task

1.3.1. Objective

Examine the possibility to detect peritonitis at an earlier stage than is possible today without direct access to the effluent fluid.

1.3.2. Requirements

This project started with the idea of tracking the increase of white blood cells (WBC) in the effluent dialysate as an indication of peritonitis. The aim was to make it simple and safe enough for the patients to administer the procedure themselves. If this idea could be implemented in the PD patients daily routine and warn them of an oncoming episode of peritonitis it would be considered an immense improvement for PD patients. To be able to implement this as something that could be available for every patient it had to be cheap. No new disposable items or modification of items involving the treatment was allowed. No direct access to the effluent dialysate was desired either. This would make the procedure complicated warranting extra work for the patient to sterilize the equipment before every measurement or demand some sort of disposable gadget.
The PD patient uses new sets of tubes and drain bags for handling incoming dialysis fluid and effluent dialysate (see Figure 1). The idea already established at Gambro was to use the existing tubes as a way of handling the effluent dialysate without the need for any new disposable items. No modification that would have any affect

on the way the tubes are manufactured was allowed. The tubes and drainbags are mass-produced to be as cost efficient as possible. Any modification would drastically increase costs since four new set of bags and tubes are used every day. Basically this meant that the tracking of the number of WBC in effluent dialysate should be done in a non-invasive way through the tube sets.

1.3.3. The general idea

To count cells or particles in a non-invasive way could be done in several ways. This diploma work focuses on an optical approach of measuring absorption or scattering of light. The way of counting particles with the aid of different scattering or absorption setups are well known (see the light scattering section, page 6). However an out of the laboratory particle counter for patient use is currently not available. The non-invasive criteria means that the plastic tube that contains and carries the effluent dialysate from the patient may not be cut open or modified in any way that would require a change in the tube's manufacturing process. Since one of the first detectable symptoms of peritonitis is an increased number of white blood cells and therefore cloudy dialysate it should be sufficient to look at the fluid. There are several methods that could be suitable for such measurements. Measuring the absorption or light scattering through the fluid could be a way of finding out how many white blood cells that reside in the effluent dialysate. The light scattering measurements was done with a laser as a light source pointed at the tube containing dialysate and a light sensitive detector. Different setups based on the idea of light scattering and light absorption for detection of peritonitis was also explored in this diploma work.

The intention was to see if it was possible to detect low and rising cell counts in effluent dialysate using non-invasive measurements in different ways. The main part of the diploma work was to test the light scattering setup made at Gambro called the GPD (Gambro Peritonitis Detector). Other methods were sporadically tested but the setup that carried the most expectations was the GPD.

The GPD should preferably be able to track cell concentrations of 0 cells/µl up to 100 cells/µl and also be able to determine if the cell concentration is above 100 cells/µl.

Analysis methods involving light scattering of cells uses, most often, techniques adapted for a laboratory environment. The circumstances under which the GPD is supposed to function are quite different from those in a laboratory. The GPD should be able to measure on the effluent dialysate through a PVC tube affecting the light scattering without the possibility of any sample preparation often made in laboratories. The GPD doesn't have to make detailed analysis of the dialysate. It only has to detect the increase of particles in the effluent dialysate and warn the patient. The warning

should motivate the patient to seek help for further analysis of the effluent dialysate.

Theoretical simulations of the light scattering in the case of the GPD setup was not considered due to limited time and the precedence of experimental work.

2. Methods and equipment

2.1. Gambro peritonitis detector (GPD)

2.1.1. Setup

The GPD was created by Hans Hallstadius at Gambro. It basically consists of a light source and a light detector. The light source used was a class 1 laser (see appendix) with a wavelength of approximately 635 nm. Different lasers were found to have different laser profiles. As will be discussed later, the orientation of the oval shaped cross section of the laser beam used was important for the functionality of the GPD. The light detector used was a Hamamatsu Si photodiode with preamplification, S8745-01.

The tube through which the laser was aimed was from the tube set used with the Serena™ (see appendix). The test solutions were filled into drain bags that were connected with each other through plastic tubes. These drainbags were used to flow the fluid through the tube by having them at different heights. The reason for using a height difference and not a pump was that the pump gave a pulsated flow, which interfered with the measurements.

The flow rate of the solution varied from very low at 1 ml/min up to approximately 500 ml/min. The flow was calculated by placing one of the drainbags on a scale connected to a computer. Using a program written in Labview the flow was calculated using the change in weight during a specific amount of time. The setup is shown in
Figure 5.

The light from the laser was focused with a plano-convex lens onto the tube. The scattered light from the tube and its contents was focused through two lenses onto a photodiode. The diode recorded the scattered light and transformed it into a current, which was amplified and then transformed into a voltage. This voltage was detected and digitalized through a National Instruments DAQ-Card 6024E that sampled the signal from the photodiode with a sample frequency of 1000 Hz. The signal was stored and displayed with the aid of a program made with NI Labview (see Figure 6). The voltage values were stored in data files, which had to be converted into txt-format before analyzing them in Matlab.

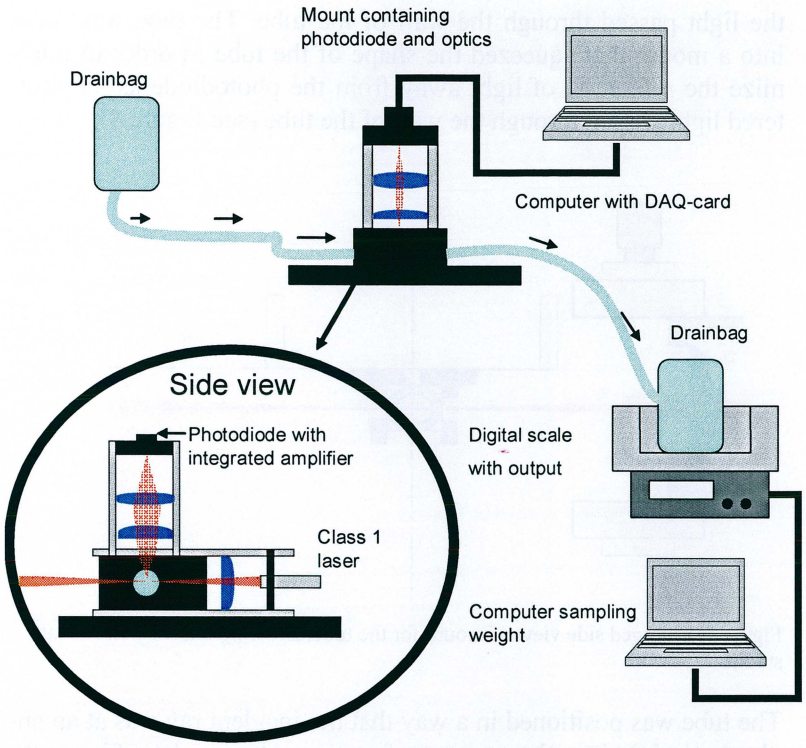

Figure 5. The setup for measurements with the GPD.

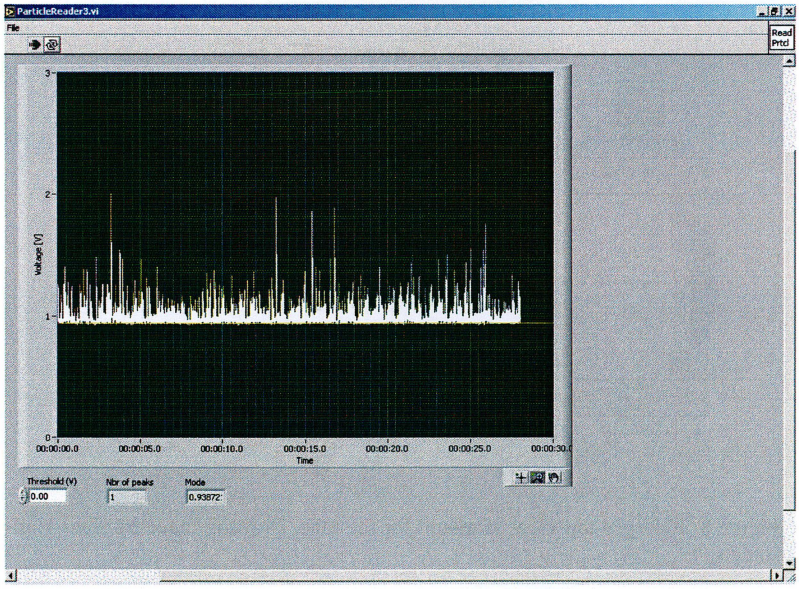

Figure 6. An example of the signal from the GPD displayed in the program made with NI Labview. The output voltage from the S8745-01 photo diode is shown as a function of time.

To be able to get as much light as possible inside the tube and in contact with the fluid a lens with a long focal length was used. This gave a long and thin focus. It also minimized the intensity loss as

the light passed through the wall of the tube. The tube was fitted into a mount that squeezed the shape of the tube in order to minimize the refraction of light away from the photodiode as the scattered light passed through the wall of the tube (see Figure 4).

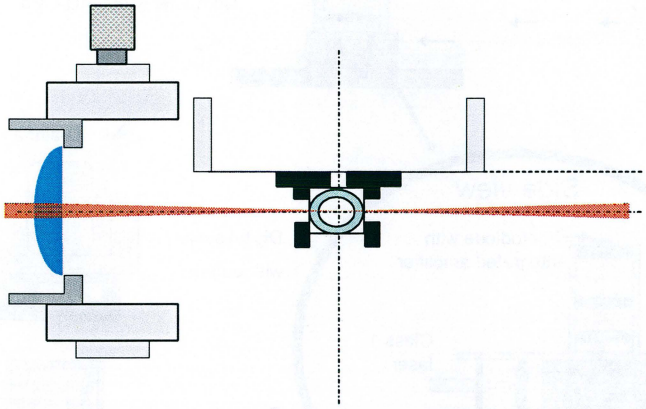

Figure 7. Enlarged side view of mount for the tube. Drawing made by Hans Hallstadius.

The tube was positioned in a way that the incident ray was at an angle that minimizes the amount of static scattering (see Figure 8). This was optimized in the lab by Hans Hallstadius and based on the empirical knowledge gained there.

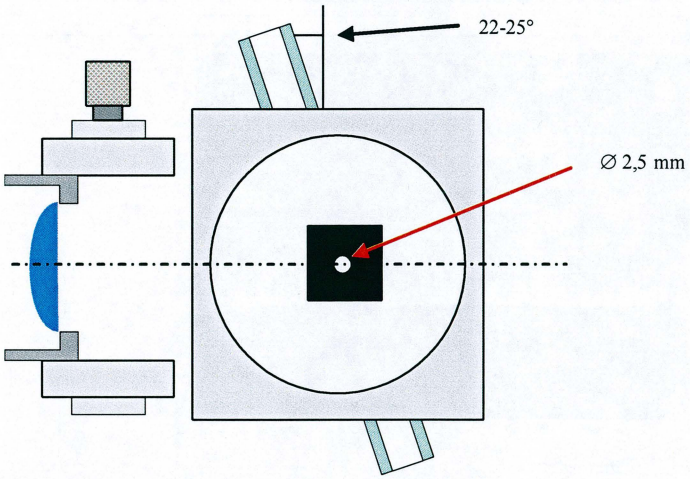

Figure 8. Enlarged top view of mount for the tube. Drawing made by Hans Hallstadius.

2.1.2. Data analysis

The sampled data was converted into txt-files and loaded into Matlab where the data was analyzed. The signal consisted of a number of peaks created as scattered light hit the detector. The National Instruments DAQ-Card 6024E sampled the signal from the photodi-

ode with 1000 Hz so that one peak lasting for example 70 ms would be built up by 70 samples in the data file.

A variety of programs were written in Matlab to facilitate the data analysis. The data files was named with the following standard naming: "c[cell concentration]f[flow].txt". For example c20f50.txt for a cell concentration of 20 cells/µl and a flow of 50 ml/min. With this naming the cell concentration and flow could be retrieved from the filename by using two functions. The functions were named getCellC and getFlow and had the variable "name", that stored the filename, as an input parameter. With help of these functions, plotting of measurement files was easily done independently of the amount of measurements. A program for plotting the signal along with the signal's histogram was also constructed (Figure 9). This could be used to reveal errors in the detector e.g. a low laser intensity, a damaged detector or a laser that pointed off axis. When any of these factors were present it could be seen as flat signal or a histogram with only one bar storing all samples. The algorithms calculating the cell concentration were implemented in the same program.

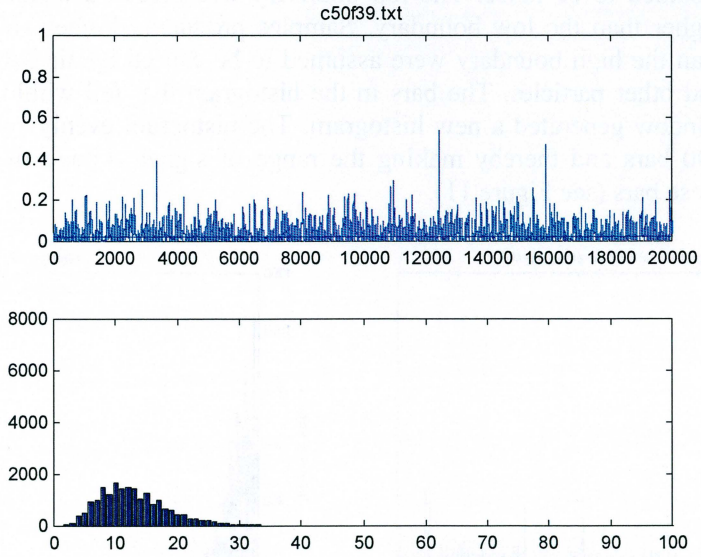

Figure 9. The GPD signal (top) and the histogram for the signal strengths (bottom).

2.1.3. The GPD algorithm

At the start of this diploma work there was already work done considering an algorithm to interpret the signal. This had been done by Olof Jansson currently working as a research scientist at Gambro.
The GPD algorithm started by loading the stored data file and transferring it into a histogram containing 500 equally spaced bars (see Figure 10).

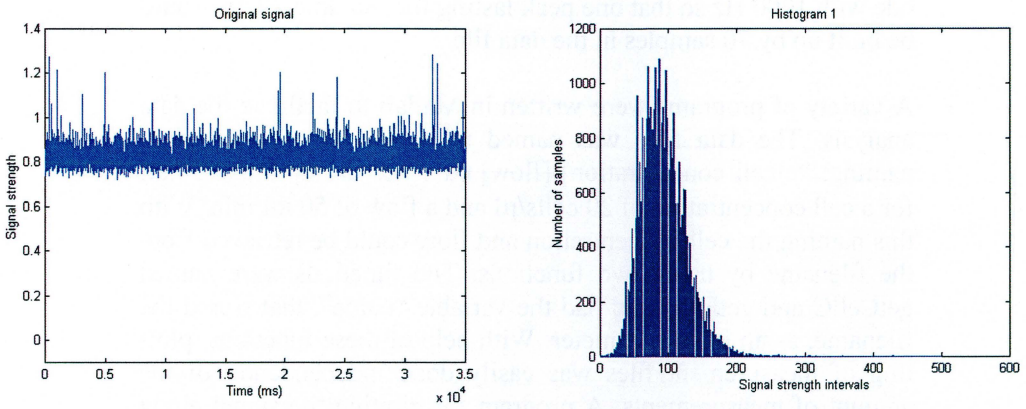

Figure 10. The original signal (left) and the original signal displayed in a histogram (right).

The signal strength for the bar containing most signal samples was identified as a baseline. The baseline was then subtracted from the signal. This lowered the entire signal. A threshold window was created based on the subtracted histogram. The low boundary of the window was positioned above the lowest signal samples that were assumed to be noise. The top boundary was placed a factor 100 higher than the low boundary. Samples producing higher voltage than the high boundary were assumed to be caused by air bubbles and other particles. The bars in the histogram that fell within this window generated a new histogram. The histogram evenly spaced 500 bars and thereby making the range of signal voltage fit into these bars (see Figure 11).

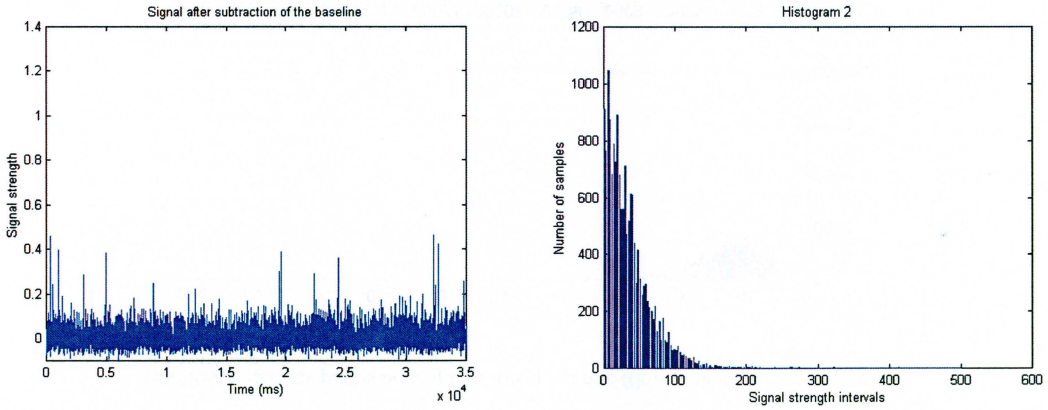

Figure 11. The signal with the baseline subtracted plotted (left). The subtracted signal modified with the threshold window is shown plotted in a histogram (right).

The algorithm assesses the histogram by starting at the lowest signal strength and continuing upward the bars in the histogram. When 80 % of all the samples were counted the algorithm checked which signal strength it had reached. The value of 80 % is an empirically acquired number by Olof Jansson that was based on his experience gained from working with the analysis of these signals. The value

80 % seemed to give the most reproducible result for different cell concentrations. A variable named chk_point was assigned the signal strength reached at the 80 percentile mark. The flow and the chk_point variable were then used in a regression curve created by previous measurements. The value found in the regression curve for this chk_point value gave an answer of the cell concentration.

2.1.4. The peak counting algorithm

Apart from the algorithm written by Olof Jansson at Gambro a new algorithm was written. This algorithm was tested for its ability to interpret the signal generated by the GPD and thereby how accurate it could determine the cell concentration in effluent dialysate. The algorithm was written so that it counts peaks in the signal arising from light scattering material passing through the laser beam. Example of this can be seen in Figure 12. One second is shown and as the signal from the GPD is sampled with 1 kHz the signal during this second is built up by 1000 sample points.

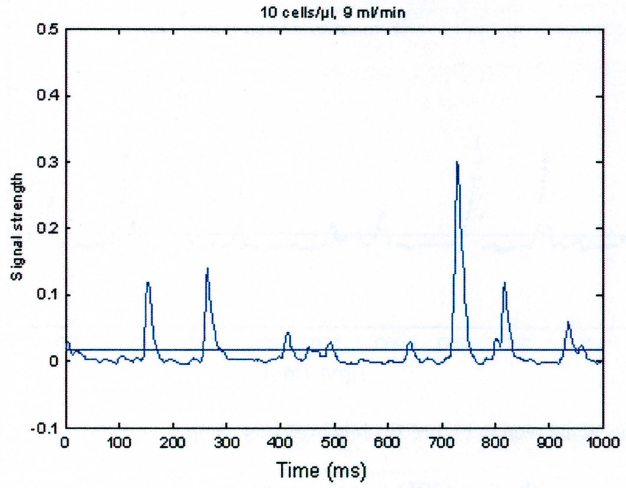

Figure 12. Peaks in the signal arising from scattering material passing through the laser beam.

If a particle in the fluid passed directly through the laser's focal point it would give a stronger signal than a particle that was partly illuminated. There was also a higher probability for it to scatter more photons during a longer period of time since the fully illuminated particle used its entire diameter as it passed through the laser beam. This meant that the fully illuminated particle would produce a larger and longer peak in the signal than the one that was partly illuminated. Since every peak was built up from single sample points it meant that there could be big differences in the number of sample points generated in different measurements depending on where in the plastic tube the laser beam was aimed. The concentration of particles in a flowing fluid varied in different areas of the flow. This phenomenon is called "The tubular pinch effect" [18] and is discussed more in detail in the discussion section on page 47. To get a

fair representation of the amount of particles that passed through the laser beam it was disadvantageous to directly correlate the amount of single samples above a certain threshold to the cell concentration. Every peak could be built up by several sample points (see Figure 13). Instead a threshold was chosen from empirical tests of what threshold level that would give best results. The threshold can be seen in Figure 12 and Figure 13. Every time the signal went above this threshold one peak was added to the peak counting variable. No more peaks were added until the signal has again been below the threshold. The algorithm also compensated for different flows with a flow dependence of flow$^{0.3}$ (see Figure 33) and for the time that a measurement lasted.

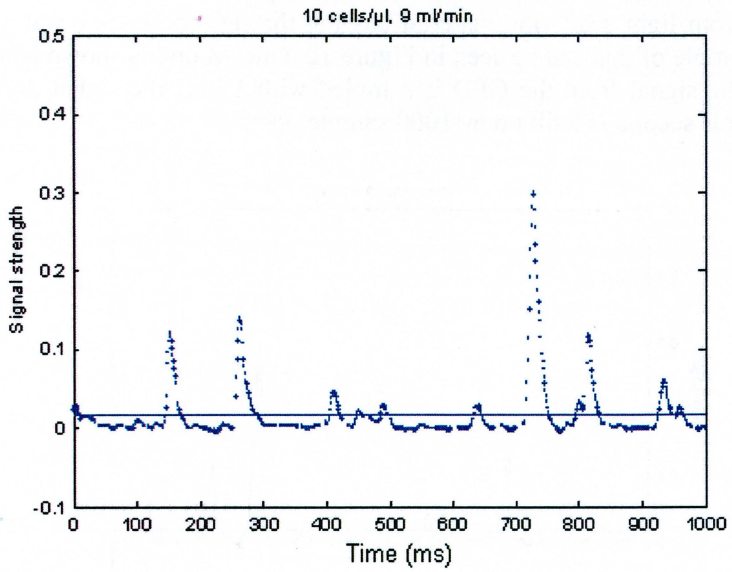

Figure 13. The signal seen in Figure 12 showing every sample.

Measurements with the GPD were made on dialysate solutions containing 1-, 5-, 8-, 15- and 18 cells/µl. The cells used were L929 mouse fibroblasts cultivated at a cell laboratory. For each cell concentration, flows ranging from 4 ml/min to 134 ml/min were used. The preparation of the samples started with a highly concentrated solution of L929 cells. The concentration was measured once with the NucleoCounter™ (see appendix). The samples were then prepared in different concentrations by diluting the concentrate with dialysis fluid. The cell concentration of these diluted samples were not confirmed with the NucleoCounter™. Later the knowledge was gained that a confirmation always should be done. The cell concentrations in the diluted samples was not always what one expected.

The peak counting algorithm showed accurate results using flows ranging from approximately 1-80 ml/min and cell concentrations up to 20 cells/µl. A combination of the GPD algorithm and the peak counting algorithm was implemented. In this algorithm the idea was

to keep track of variations in cell concentrations up to 20 cells/µl using the peak counting algorithm and then using the GPD algorithm for higher cell concentrations. The combined algorithm calculated a result from the peak counting algorithm and a result from the GPD algorithm. These two results were then compared. If the GPD algorithm produced a result higher than 20 cells/µl it was regarded as the final answer. In any other case the peak counting algorithm would give the final answer.

2.1.4.1. Data analysis

The data was acquired by an A/D-card and therefore the digital signal had discreet steps. The steps in the signal could be smoothed to facilitate the ability to discriminate the peaks with help of a filter (see Figure 34). The filter traversed the signal and took the mean of five measurement samples as a new value.

2.1.5. Attempts to increase the GPD's sample frequency

The photodiode used had a sample frequency ranging from 10 to 40 Hz depending on the amount of photons reaching it. A high level of incoming photons lowered the sample frequency and a low level has the opposite effect. The peaks generated from light flashes when cells were passing through the focus of the laser at high flow were therefore not as noticeable as the peaks obtained at lower flows (see Figure 14 and Figure 15).

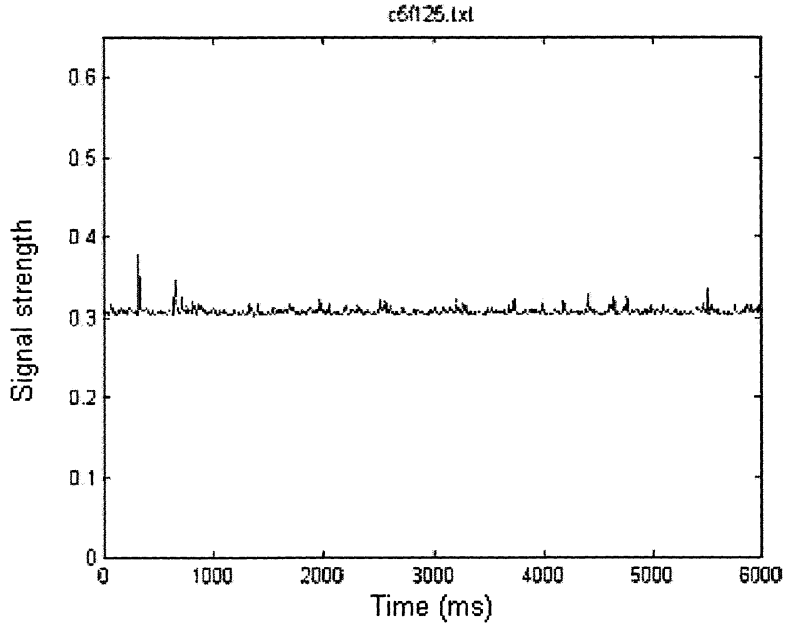

Figure 14. High flow measurement with the GPD during 6 seconds at a flow of 125 ml/min and a cell concentrations of 5 cells/µl. The signal peaks got less defined for higher flows.

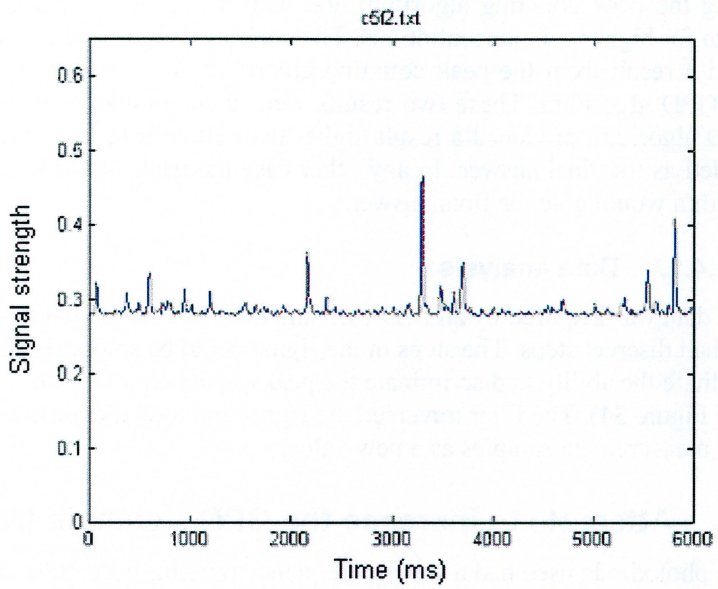

Figure 15. Low flow measurement with the GPD during 6 seconds at a flow of 2 ml/min and a cell concentrations of 5 cells/µl. For low flows the signal peaks got sharp and well defined.

There was a possibility to alter the sample frequency by connecting an external feedback resistor between the pin on the photodiode carrying the signal current and the pin connected to the photodiode's preamplifier. A resistor box was constructed (see Figure 16) with the aim to be able to increase the externally connected feedback resistor in discrete steps and in this way vary the sample frequency of the detector. The resistance could be varied from 100 MΩ up to 600 MΩ in steps of 100 MΩ. This corresponded to a sample frequency from 110 Hz down to 40 Hz. A disadvantage of increasing the sample frequency was that one at the same time got a lower amplification of the received signal (see Figure 17).

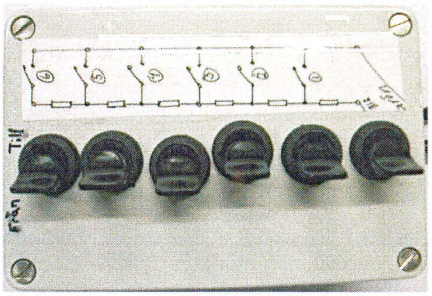

Figure 16. The resistor box used to alter the sample frequency of the detector. By using the on and off buttons on the resistor box, the sample frequency could be varied without soldering on the photodiode's pins every time a new sample frequency was desired.

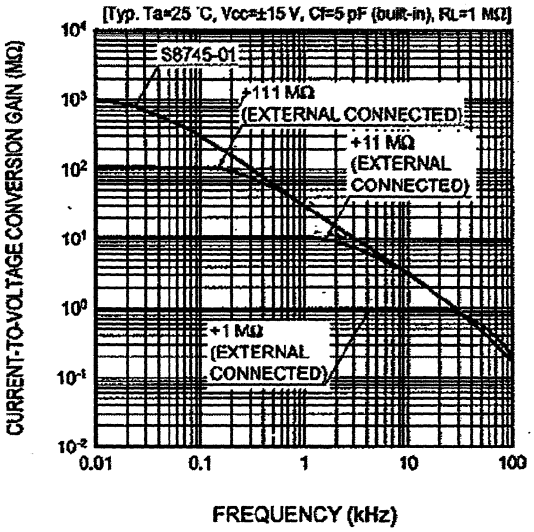

Figure 17. Frequency-gain characteristics for the photodiode S8745-01 [19] used in the GPD.

With this device connected between pin 4 and pin 6 on the detector a strong 50 Hz disturbance was picked up. The cables used, drawn from the box to the photodiode, were replaced by coaxial cables and the inside of the box was covered in aluminum foil in the attempt to create a Faraday cage. This decreased the disturbance but it was still noticeable.

2.1.6. Low flow measurements

Dialysate from a patient recovering from peritonitis was found to have 210 cells/µl using a microscope and a Bürker chamber (see section 9.2). The dialysate was diluted in steps ranging from 10 – 210 cells/µl. This was done by weighing dialysate and then adding a calculated amount of pure dialysis fluid to obtain the desired cell concentration. Low flows ranging from 5 – 100 ml/min were used during the measurements with the GPD. The cell concentration calculated by the dilution factor was taken as the true cell concentration. During this measurement, occasional measurements on higher flows were also made.

2.1.7. High flow measurements

A concentrated solution of L929 cells was diluted with dialysis fluid to the following concentrations: 10-, 25-, 40-, 80- and 120 cells/µl. This was done by weighing pure dialysis fluid on a scale, pouring it in a sterile drain bag and then adding the newly stirred cell concentrate into the drain bag. A control of the cell concentration was made using the NucleoCounter™ and the mean of three measurements with the counter was taken as the true cell concentration. Flows ranging from 200-500 ml/min were used.

2.2. Two-dimensional scattering measurements

The ability of measuring on a not flowing volume of the effluent dialysis solution was tested. The main components used were a Hamamatsu C8484-05G CCD camera and a class 1 laser with a wavelength of approximately 635 nm. To illuminate a larger volume a laser sheet was created with the aid of a cylindrical lens. The mount fixated and squeezed the tube so that the side facing the camera was as flat as possible to minimize distortion of the picture. Figure 18 shows the two-dimensional scattering setup.

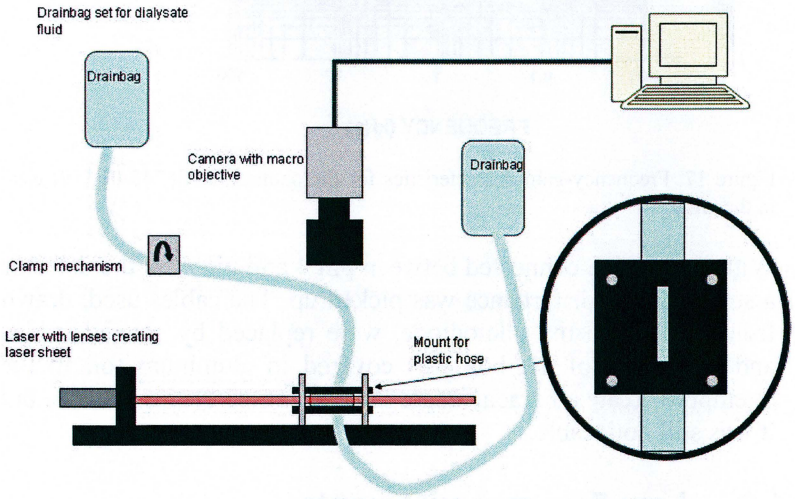

Figure 18. Schematic drawing of two-dimensional scattering setup.

The scattered light from particles in the tube travels through the slit in the mount and is focused onto the CCD-chip in the camera through the macro lens objective. The camera was connected to a IEEE1394 PCI card in a desktop computer through a FireWire cable. The acquired pictures were stored in the software program Wasabi, made by Hamamatsu. Figure 19 shows the equipment used.

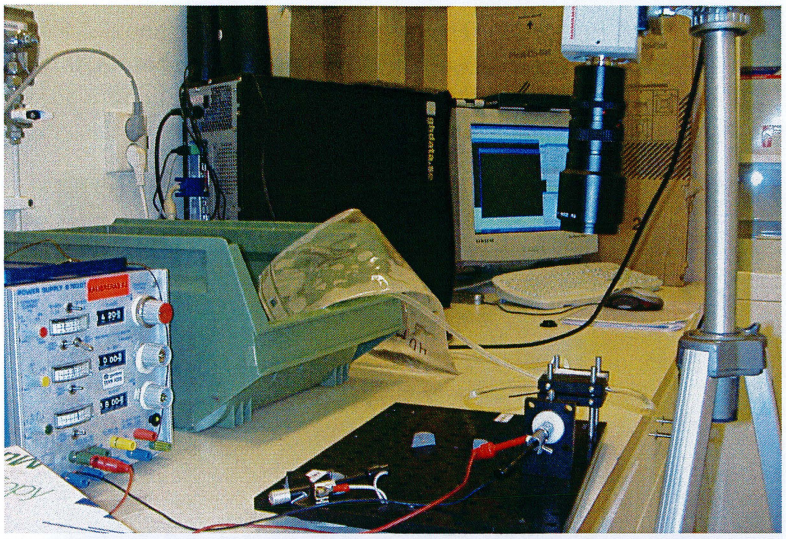

Figure 19. Equipment for two-dimensional scattering measurements.

The camera was mounted on a tripod. The mount for the tube, the laser and optics were all secured on a bench. Figure 20 shows the two-dimensional scattering setup in its operational mode.

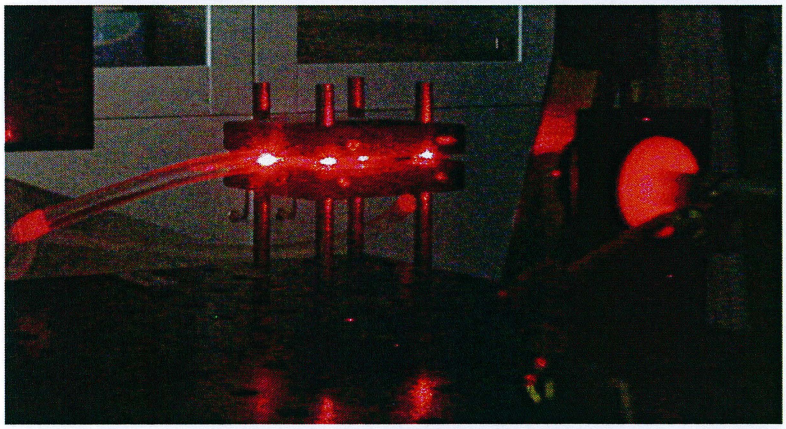

Figure 20. Mounting piece and laser setup for two-dimensional scattering measurement showing the laser sheet focused on the tube.

The camera was focused onto the tube. When a sufficiently sharp picture was obtained the measurement could start. The camera started to take a predetermined sequence of pictures. During that time the flow of the fluid would be turned on and off manually. This created different sample volumes of which the camera took pictures. These pictures were later modified in the software programs Wasabi and Matlab. In Wasabi the picture would first be adjusted to show the intensity range where the small dots of scattered light coming from cells, bubbles or particles would be the most evident. The camera created a 16 bit grayscale picture. The intensity range of interest could be transformed by a tool in Wasabi that showed the intensities in the picture as a histogram distribution. The pictures were then transformed into 8-bit grayscale pictures

(Figure 21 and Figure 22). The original pictures were about 2.5 MB each and a short film sequence of 180 pictures was about 370 MB. In Wasabi a background subtraction was also made to eliminate all the static signals in the picture (see Figure 23).

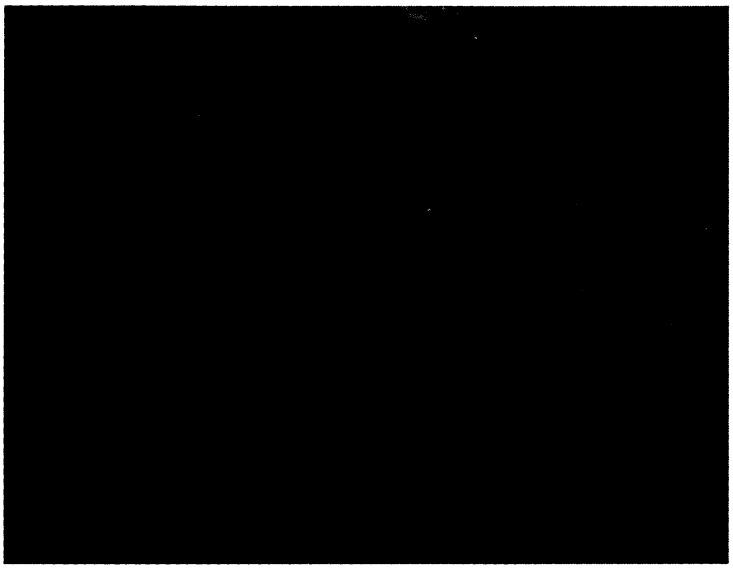

Figure 21. Picture taken by the camera reduced to an 8-bit format. The picture is of a sample with a cell concentration of 130 cells/µl.

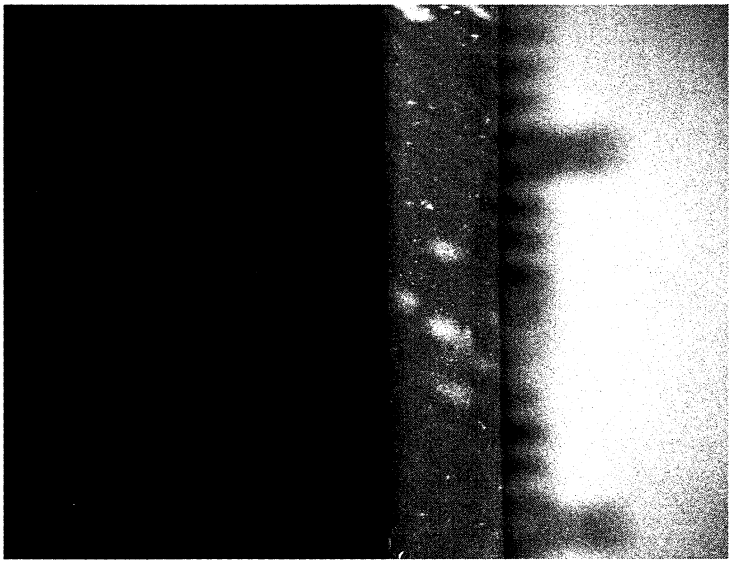

Figure 22. The same picture as in Figure 21. The dynamic range of the intensity in the picture has been adjusted to more clearly show the light coming from the tube.

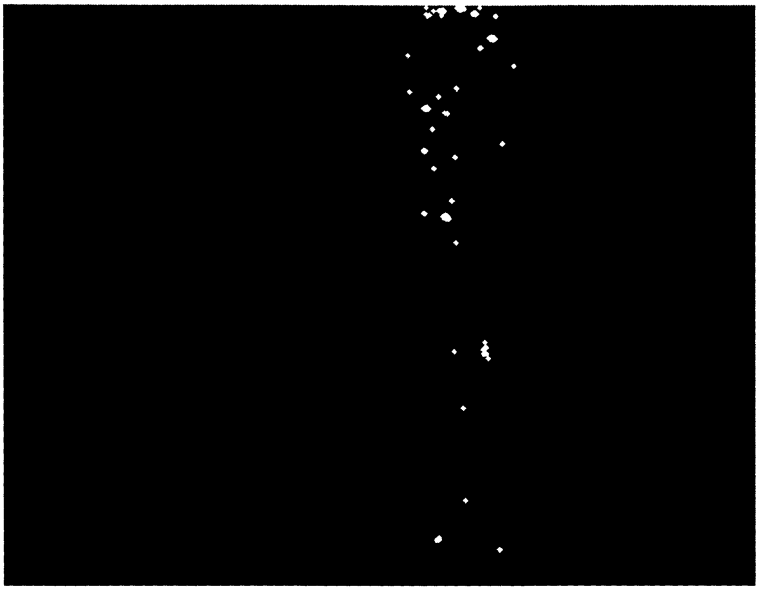

Figure 23. Picture of the same volume as in Figure 22 but with a background subtraction made. The tiny white spots could be detected as cells or air bubbles. The picture has been further filtrated after analysis with a sharpen and enlargement filter to make the spots more evident for the reader.

After the subtraction and modification the pictures were loaded into Matlab. An area of approximately 10x3 mm was targeted in each picture. This would be the area in the picture that would be examined.

Due to the difficulties of having an improvised setup the magnification of the area differed somewhat between the different measurements of different cell concentrations. This occurred because the setup had to be moved and thereby put out of focus to be able to replace the fluid bags. To compensate for the difference in magnification the result was divided by the image area i.e. the number of pixels the area in the tube consisted of.

The CCD-chip in the camera consisted of a 1.37 million pixels 6.45 μm x 6.45 μm in size [20]. The grayscale picture generated by this camera was mathematically described as a matrix. Each cell in the matrix represented one pixel. The cell contains a numeric value that was normalized to fit a certain standard. Usually the number 1 means that the pixel has the highest intensity possible i.e. it is white and the number 0 means that the pixel is black. It was with these values the picture was analyzed. A mean value of the intensity in the examined area of the picture was taken. A threshold value was created in a percentage relation to the mean value of the image area. Any pixel with an intensity value higher than the designated threshold value was counted. The total number of counts i.e. high intensity pixels, was divided by the total number of pixels in the analyzed area. This was done for each picture in the sequence. The number of pixels above the threshold value was then plotted.

Every film was examined to determine for which picture in each sequence the flow was at a standstill. This was done to avoid counting the signals generated when the camera filmed a flowing solution. Each film sequence of every cell concentration contained 1-4 different standstill samples of which an analysis was made. The relation between these high intensity pixel counts and the cell concentration is presented in the result section (Figure 46 and Figure 47).

When the tube was squeezed into the mount of the setup the cross-section of the tube was approximately 14.5 mm^2. A 30 mm long section of the tube in this mount contains approximately 0.435 ml. The section used in the analysis was approximately 10 x 3 mm which gave a volume of 0.080 ml. However it was only the part illuminated by the laser that could be registered. The laser sheet was approximately 0.15 mm thick which gave a sample volume of 4.5 µl. This was the volume used in the data analysis of the pictures. Every time a new clamp and measure procedure was made new dialysate flowed into the designated area and thereby making it possible to observe a new sample.

2.3. Absorption measurements

In the beginning of the project the possibility of using absorption for detection of peritonitis was tested. The aim was to see if it was possible to detect sensible quantities of albumin i.e. the amount that would appear in dialysate, and if such analysis could be made through the plastic tube. Peritonitis is often associated with substantial loss of serum albumin in the body and therefore an increase in the effluent dialysate [21]. Absorption spectra were acquired for different cell concentrations of the cell type L929. Absorption spectra for the PVC tube were recorded to determine for what wavelengths the tube would be transparent.

The wavelength-dependent absorption measurements were made with a PerkinElmer Lambda 20 spectrometer. The absorbance A was defined as the logarithm of the quotient between the intensity of the reference beam and the sample beam.

$$A = \log \frac{I_{ref}}{I_{sample}}$$

3. Results

3.1. GPD measurements

3.1.1. High flow measurements with the GPD algorithm

The results from the high flow measurements with the GPD are presented along with the result from the NucleoCounter™ in Figure 24. The samples shown are the mean of three samples from the GPD and NucleoCounter™ respectively. The later method gives a slight variation in result when measuring on the same sample. This variability was studied as a comparison to the variability in results from the GPD.

The aim was to measure on 0, 10, 25, 40, 80 and 120 cell/µl but the results from the NucleoCounter™ showed that the cell concentration obtained was slightly different from the one calculated by the dilution factor (see discussion).

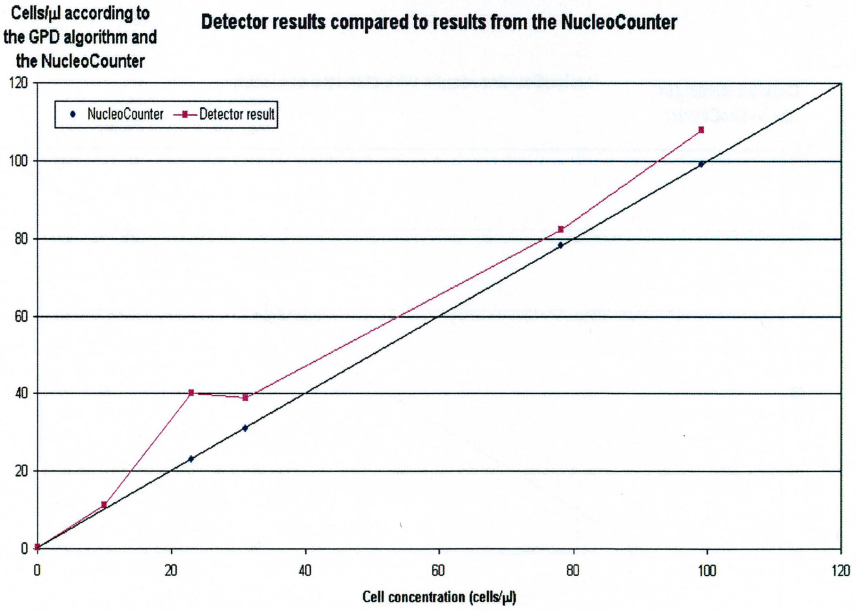

Figure 24. The results from the GPD compared to the results from the NucleoCounter™. The samples shown are the mean of three samples from the GPD and NucleoCounter™ respectively. The samples at 0 and 10 cells/µl could not be measured with the NucleoCounter™ as it had a lower detection limit of 15 cells/µl. At these points only the results from the detector are presented.

A variation in results was expected and as a comparison, the standard deviation for results from the detector and results from the NucleoCounter™ are plotted in Figure 25 and Figure 26.

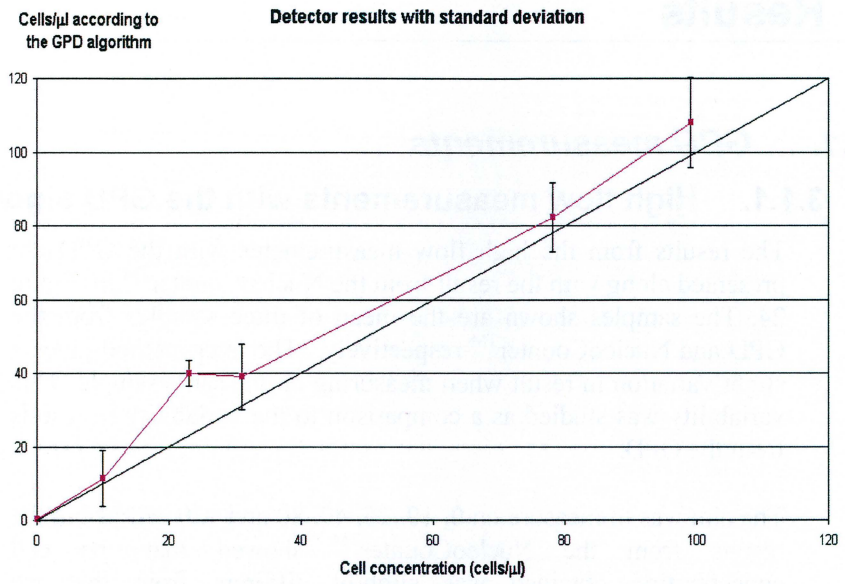

Figure 25. The results from GPD with standard deviation. The cell concentration used as a reference was measured with the NucleoCounter™.

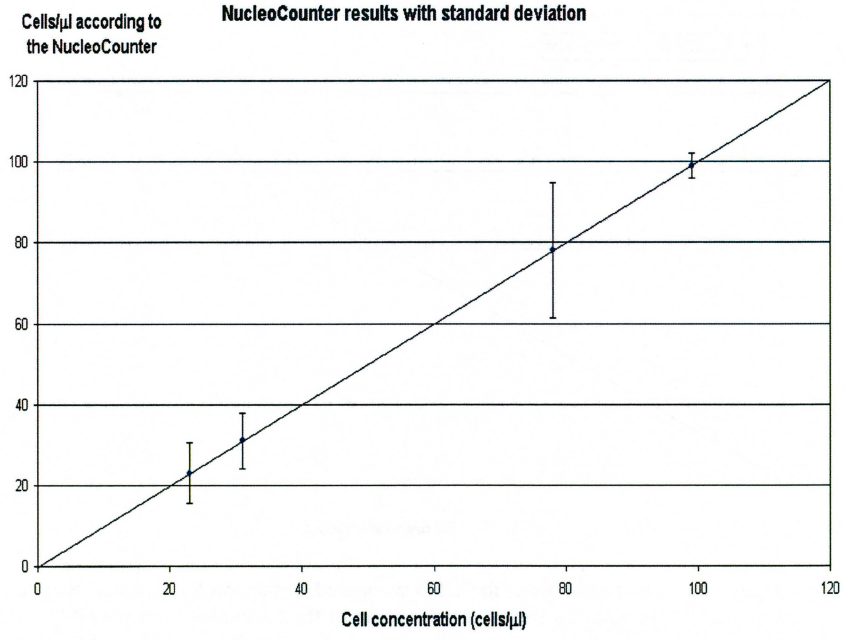

Figure 26. The results from the NucleoCounter™ with standard deviation.

3.1.1.1. Using the GPD without the Serena™

The GPD algorithm uses the flow as an input parameter. The flow dependence was found to be flow$^{(-1/3)}$. If the draining of dialysate in CAPD is between, lets say 150-350 ml/min, the flow compensation

factors will be between 5.3 and 7.0. These factors differ with 32%. This might be an acceptable error margin to count with when following the variation in cell concentration in CAPD where the flow isn't monitored. In Figure 27 the result from the high flow measurements when assigning the flow a constant value of 350 ml/min (which corresponds to a flow compensation factor of 7.0) are presented. This figure should be compared to Figure 24 and Figure 25 where the exact value of the flow (ranging from 200-500 ml/min) was used.

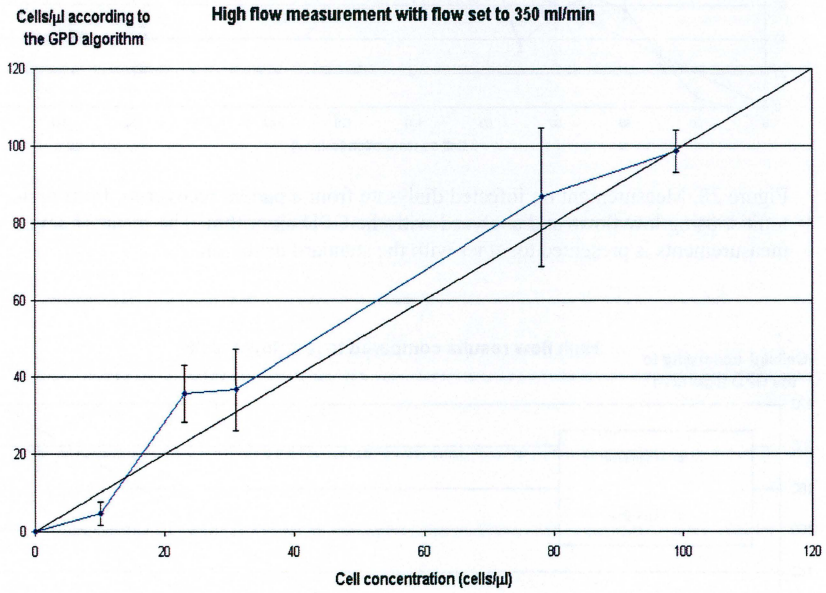

Figure 27. High flow measurements using flows in the range 200-500 ml/min. The flow parameter was set to a constant value of 350 ml/min in the GPD algorithm. The mean of three samples is presented along with the standard deviation. This figure should be compared to Figure 25 where the exact value of the flow was used.

3.1.2. Low flow measurements with the GPD algorithm and the peak counting algorithm

In Figure 28, the results using the GPD algorithm on low flow measurements are presented for different cell concentrations. Results showing single measurements samples (not the mean of several) using low flows in the range 15-30 ml/min are plotted along with results using high flows in the range 156-260 ml/min in Figure 29.

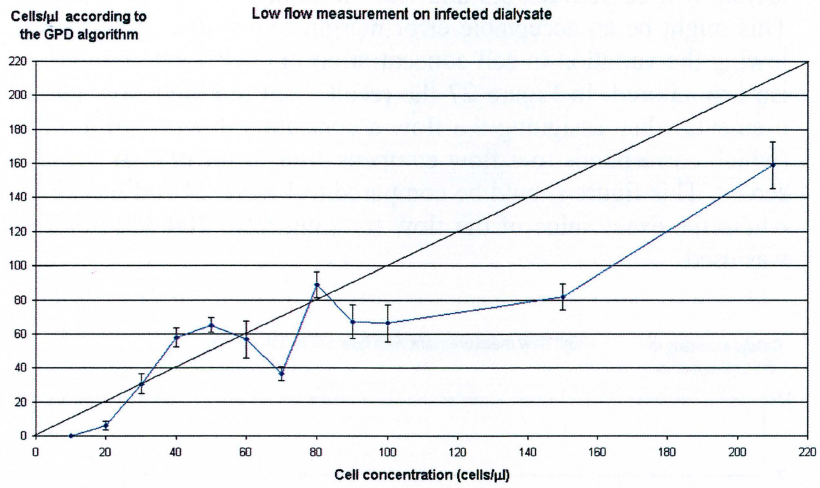

Figure 28. Measurement on infected dialysate from a patient recovering from peritonitis, using low flows and analyzed with the GPD algorithm. The mean of seven measurements is presented together with the standard deviation.

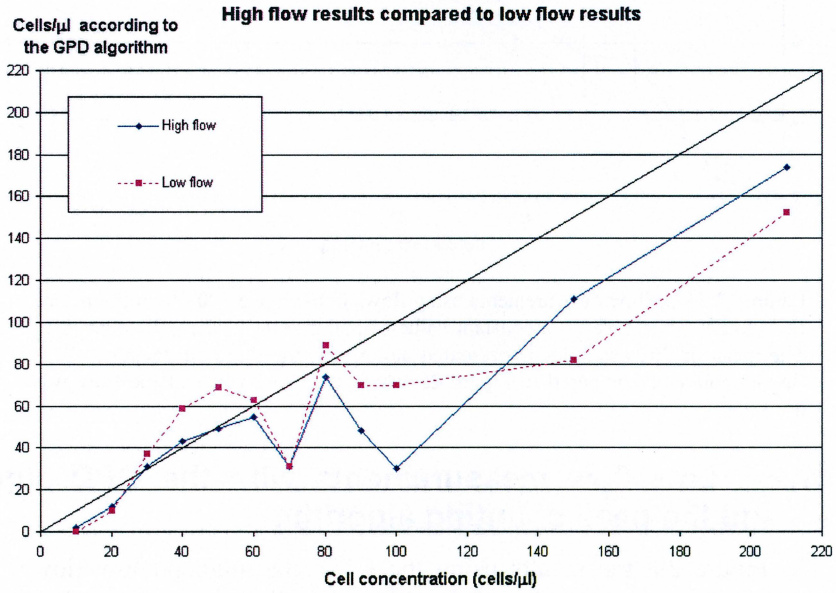

Figure 29. High flow results compared to low flow results using the GPD algorithm. Single data samples are used and not the mean value of measurements as plotted in Figure 28.

3.1.3. The peak counting algorithm

Results from the peak counting algorithm when measured on L929 cells are presented in Figure 30. The cell concentration in the samples was calculated by diluting a known cell concentration verified with the NucleoCounter™.

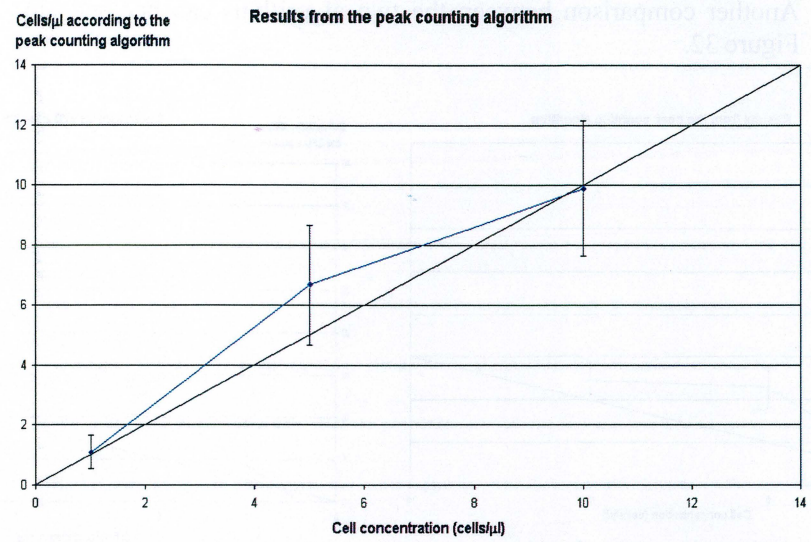

Figure 30. Results from measurements analyzed with the peak counting algorithm. Flows ranging from 1-50 ml/min.

3.1.3.1. Comparison between the GPD algorithm and the peak counting algorithm

In Figure 31 the results from the peak counting algorithm is shown with their standard deviations. In the same figure results from the GPD algorithm can be found. The results are plotted as a function of cell concentration calculated by dilution.

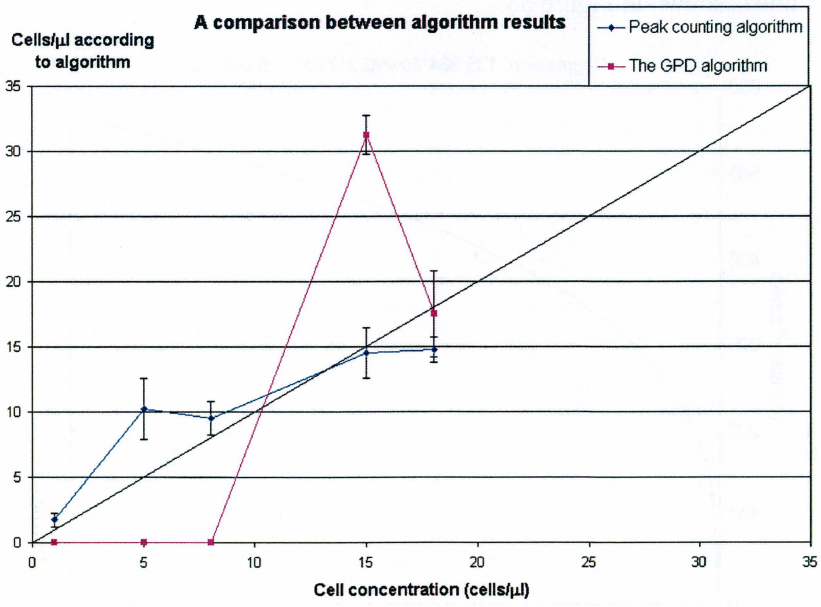

Figure 31. Results from the measurements with the detector using the peak counting algorithm (dots) compared to results using the GPD algorithm (squares).

Another comparison between the two algorithms can bee seen in Figure 32.

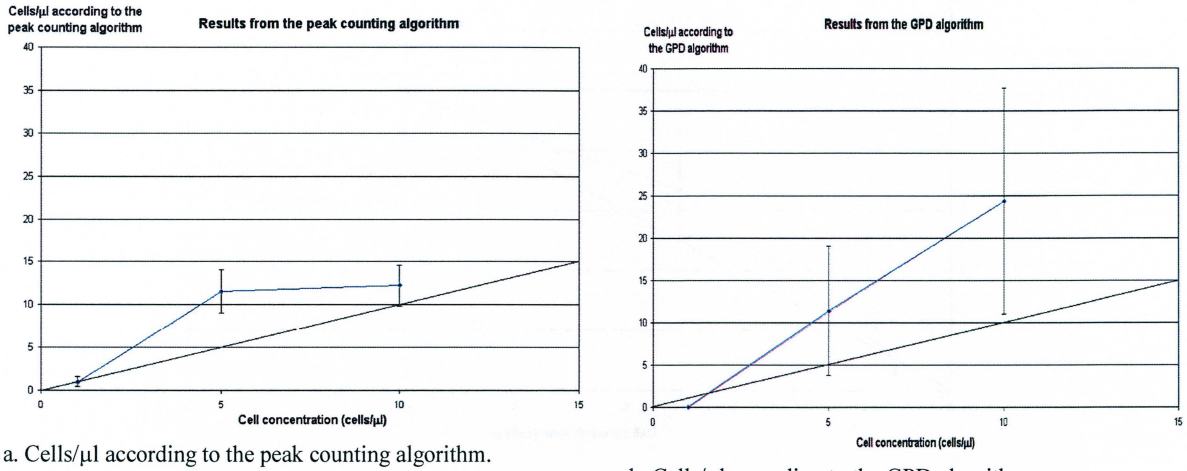

a. Cells/µl according to the peak counting algorithm.

b. Cells/µl according to the GPD algorithm.

Figure 32. The result from the peak counting algorithm (a) compared to results from the GPD algorithm (b). Flows ranging from 1-50 ml/min were used and the cell concentration for every sample was measured with the NucleoCounter™. The mean from seven samples are presented with the standard deviation.

3.1.3.2. Data analysis

As mentioned in the methods section, there has to be a compensation for different flows in the algorithm. The flow dependence in the peak counting algorithm was found to be flow$^{0.3}$. An example of this is shown in Figure 33.

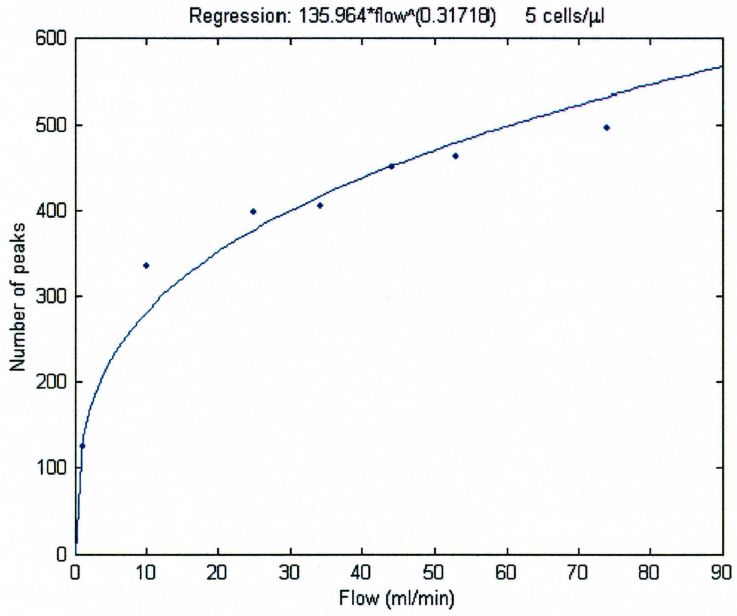

Figure 33. The flow dependence in the peak counting algorithm. The number of peaks is plotted against the flow for a cell concentration of 5 cells/µl. The regression that best fitted the data samples was 135.963*flow$^{0.31718}$.

To overcome the problem that the digital signal has discrete steps a filter was used. This problem existed for weak signals when measuring on very low cell concentrations. The effect of the filter can bee seen in Figure 34.

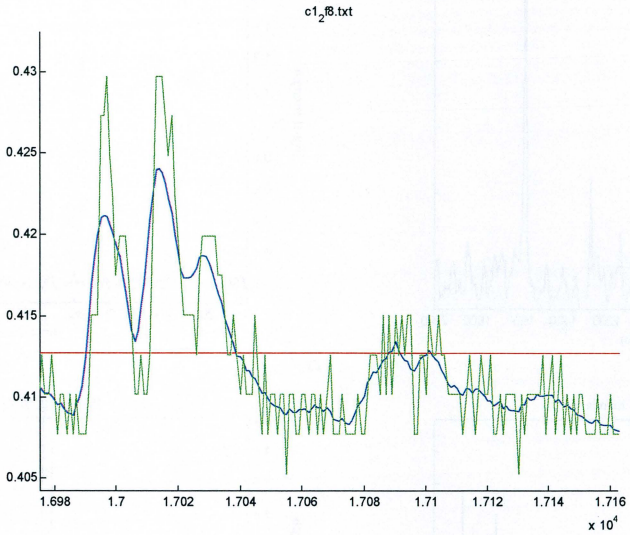

Figure 34. Raw data (green) plotted together with the mean (red) and sliding mean (blue) of the raw signal. The measurement was made with a cell concentration of 1.2 cells/µl and a flow of 8 ml/min.

3.1.4. The GPD signal dependence of laser orientation

As will be discussed in the section of sources of errors section there was a dramatic change in the signal's appearance when the lasers oval shaped spot was orientated in different ways. In Figure 36, a comparison between signals when having the laser positioned in a 10° angel from the vertical plane (Figure 35a) and when orientated horizontally (Figure 35b) is presented for different flows and a cell concentration of 152 cells/µl.

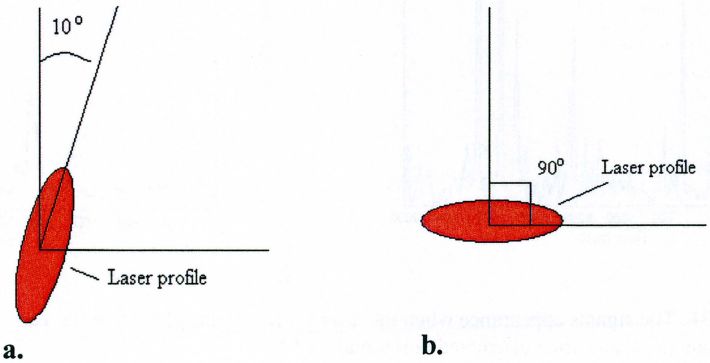

a. **b.**

Figure 35. The laser has an oval shaped profile and the figures above show a cross section of the laser. A 10-15° angel was found to be the best orientation of the laser (a). With the laser profile orientated horistotally the GPD signal was affected dramaticly.

The laser rotated 10° from the vertical plane (Figure 35a)

The laser orientated horizontally (Figure 35b)

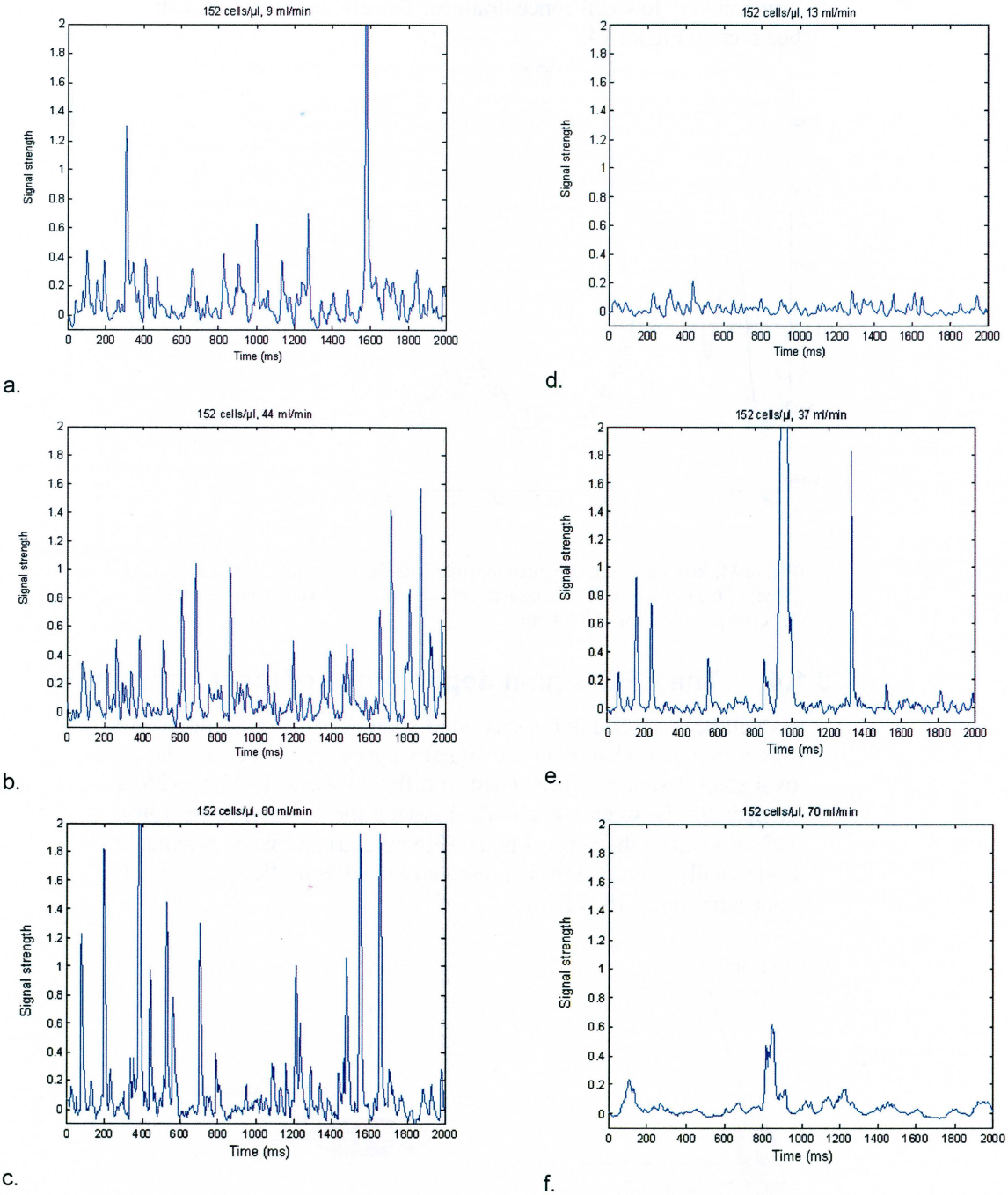

Figure 36. The signals appearance when the laser profile rotated 10° from the vertical plane (a-c) and when orientated horizontally (d-f).

3.1.5. The GPD signal dependence of air bubbles

With the GPD there were some problems involving the interpretation of the signal. One thing was how to distinguish between a cell, another particle, or a tiny air bubble. This proved difficult in pa-

tricular when implementing the peak counting algorithm with the GPD. Empirically the tests in the lab indicated that very high peaks in the signal originated from air bubbles while the more moderate peaks arised from cells and similar particles. When the drain-bag, which contained the solution, had been shaken there were a large number of air bubbles. When making a measurement shortly after the bag had been shaken the signal showed significantly more and larger peaks. When handling the drain-bags with care and mixing them calmly these peaks were reduced.

Figure 37 shows a signal plot for 5 cells/µl when bubbles are induced halfway in the measurement. The bubbles could be seen for approximately 35 seconds after the bag had been shaken.

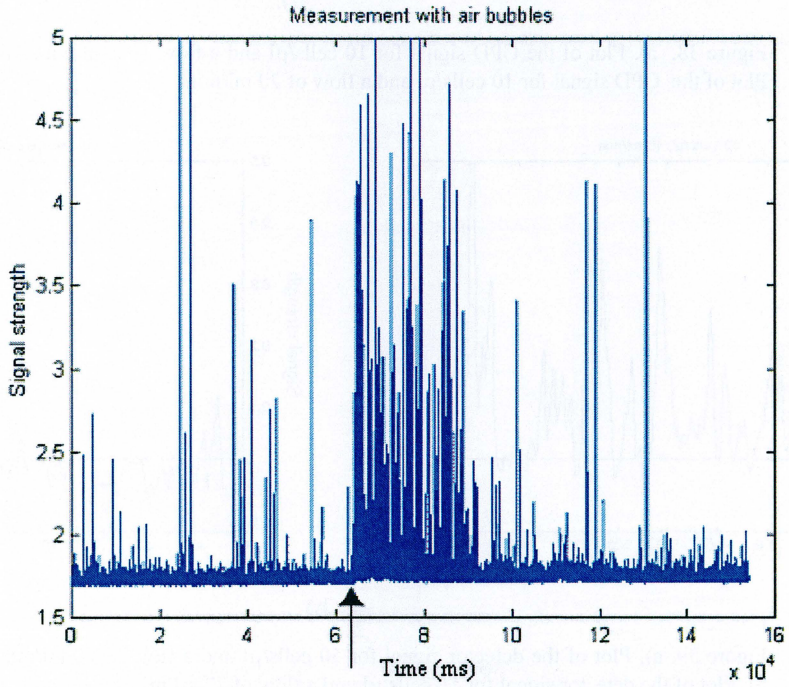

Figure 37. Signal plot with induced air bubbles. The arrow marks at what time the bag was shaken.

3.1.6. The GPD signal dependence of variation in cell concentration and flow

One could expect to see a linear dependence in the amount of peaks with an increase in flow. Raising the flow a factor seven would not give rise to seven times more peaks. Measurements were done to illustrate this. Results from such measurements are shown in Figure 38 to Figure 39.

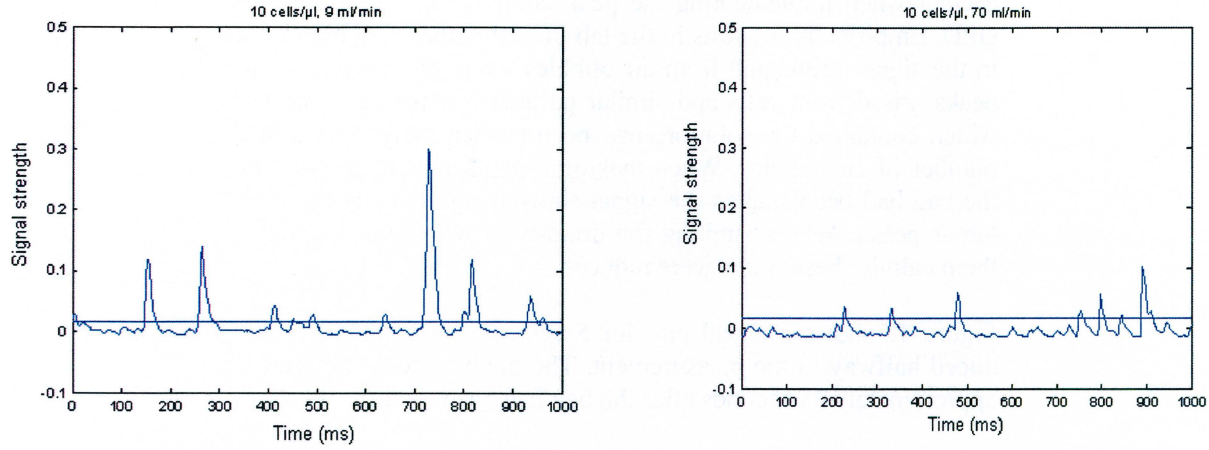

a). b).

Figure 38. a). Plot of the GPD signal for 10 cells/µl and a flow of 9 ml/min. b). Plot of the GPD signal for 10 cells/µl and a flow of 70 ml/min.

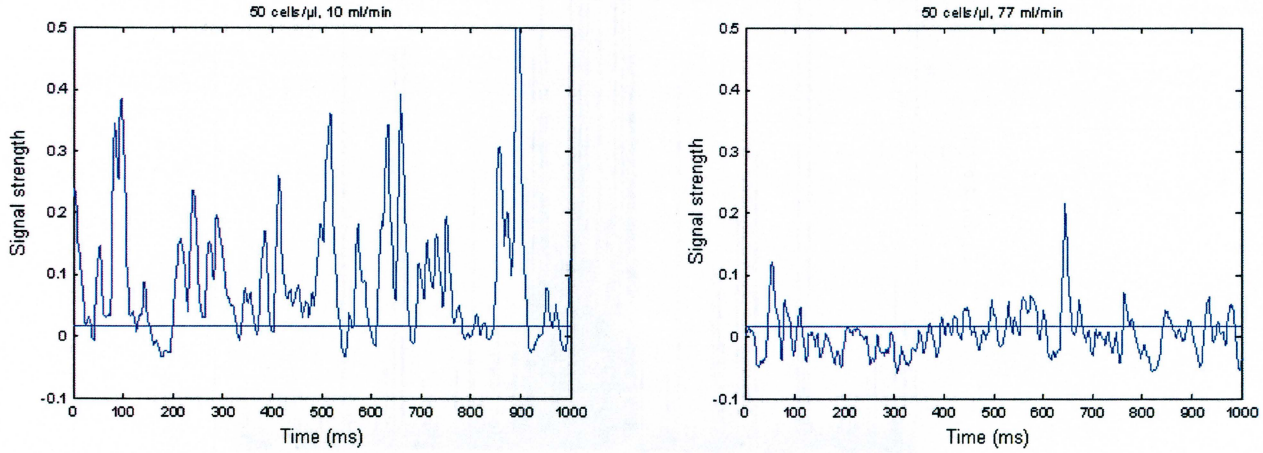

a). b).

Figure 39. a). Plot of the detector signal for 50 cells/µl and a flow of 10 ml/min. b). Plot of the detector signal for 50 cells/µl and a flow of 77 ml/min.

3.1.7. Flow dependence of the GPD algorithm

The flow dependence of the variable chk_point (the indicator for the cell concentration) used in the GPD algorithm was studied. This was done as the detector had been mounted down and conditions might have changed and also because improvements on the algorithm was sought. Some measurement results from different flows and cell concentrations are presented below along with their regression curves (Figure 40). The algorithm compensates for a flow dependence of flow$^{(-1/3)}$. The exponent takes on slightly different values for different cell concentrations but is always close to -1/3. For lower cell concentrations the regression curve becomes less consistent with the data.

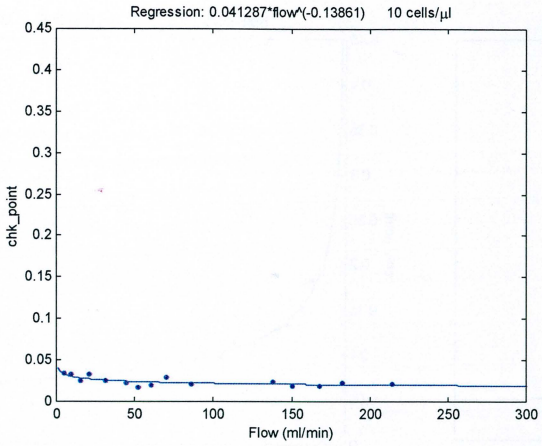

a. Cell concentration 10 cells/µl. Regression curve $0.041287*flow^{(-0.13861)}$.

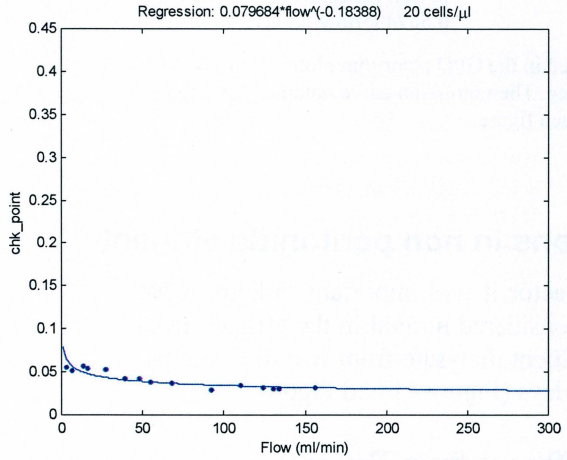

b. Cell concentration 20 cells/µl. Regression curve $0.079684*flow^{(-0.18388)}$.

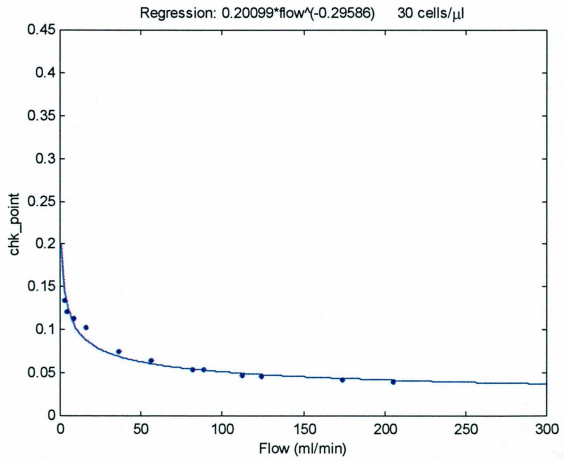

c. Cell concentration 30 cells/µl. Regression curve $0.20099*flow^{(-0.29586)}$.

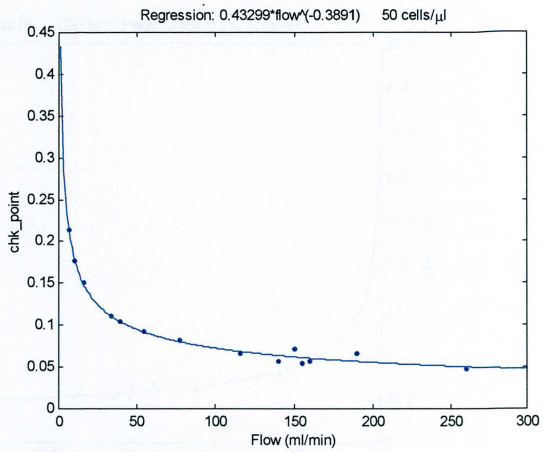

e. Cell concentration 50 cells/µl. Regression curve $0.43299*flow^{(-0.38910)}$.

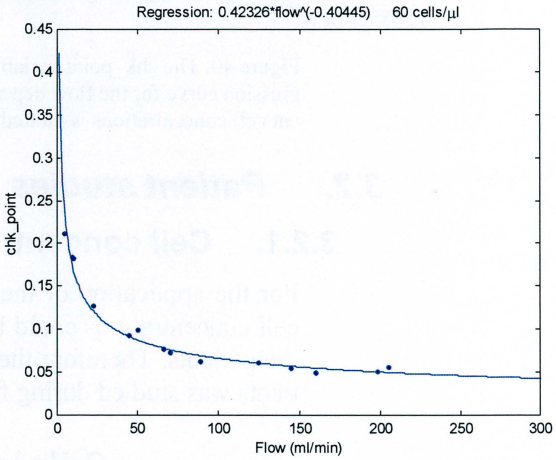

f. Cell concentration 60 cells/µl. Regression curve $0.42326*flow^{(-0.40445)}$.

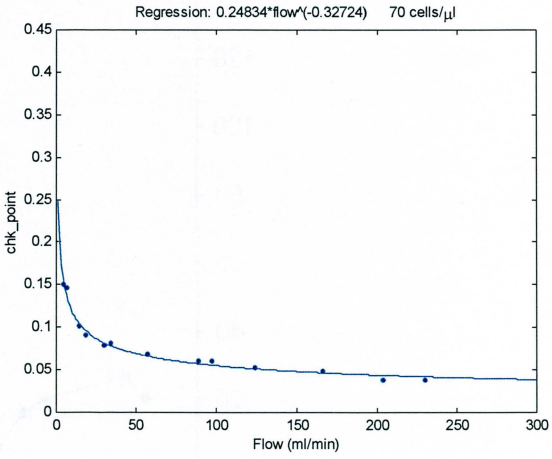

g. Cell concentration 70 cells/µl. Regression curve $0.24834*flow^{(-0.32724)}$.

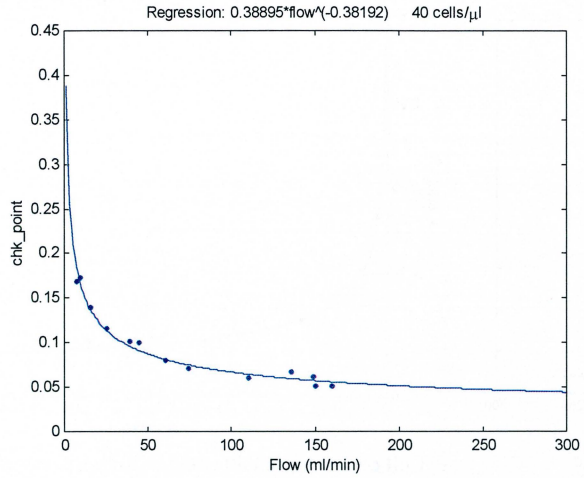

d. Cell concentration 40 cells/µl. Regression curve $0.38895*flow^{(-0.38192)}$.

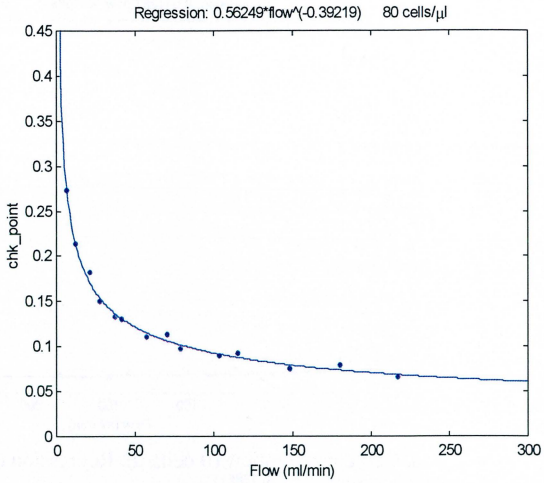

h. Cell concentration 80 cells/µl. Regression curve $0.56249*flow^{(-0.39219)}$.

Figure 40. The chk_point variable used in the GPD algorithm plotted with the regression curve for the flow dependence. The regression curve obtained for different cell concentrations is plotted in each figure.

3.2. *Patient studies*

3.2.1. Cell concentrations in non peritonitis effluent

For the application of the detector it was important to know what cell concentrations could be considered normal in the effluent from the patients. Therefore the effluent dialysate from two different patients was studied during five days (Figure 41 and Figure 42).

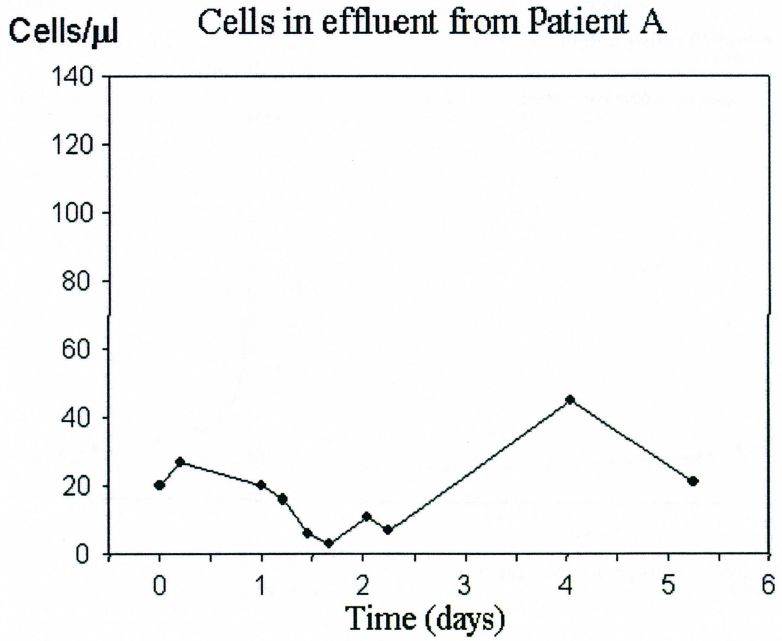

Figure 41. Cell concentration during five days in the effluent from Patient A with non-infected dialysate.

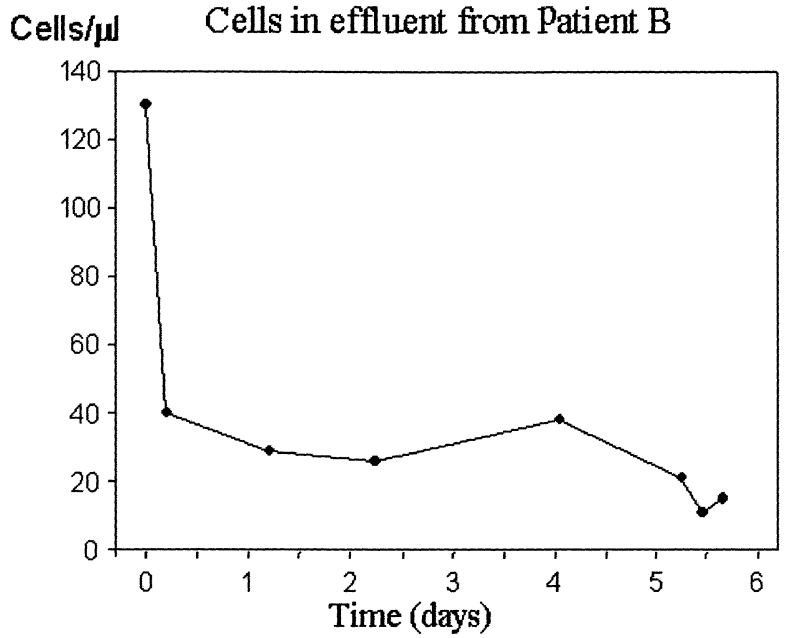

Figure 42. Cell concentration during five days in the effluent from Patient B with non-infected dialysate.

3.2.2. Cell concentrations in effluent from patients with peritonitis

Measurements of the cell concentration in effluent dialysate from patients recovering from peritonitis were made. The two figures below (Figure 43 and Figure 44) show the decrease in cell concentration while the patients were recovering from peritonitis. Day 1 represents the first day a measurement was taken from that patient and is not related to the day the peritonitis was detected. The cell concentration was calculated with the Bürker chamber. In Figure 44 the result from the GPD is presented for day 4, 8, 12 and 15. Singel results from the GPD are presented and the highest flow measurement among many was chosen. The measurement was done before the clear advantage with high flows was discovered and even higher flows had been desired with knowledge of that. Table 1 shows the flows that were used for the GPD-measurement.

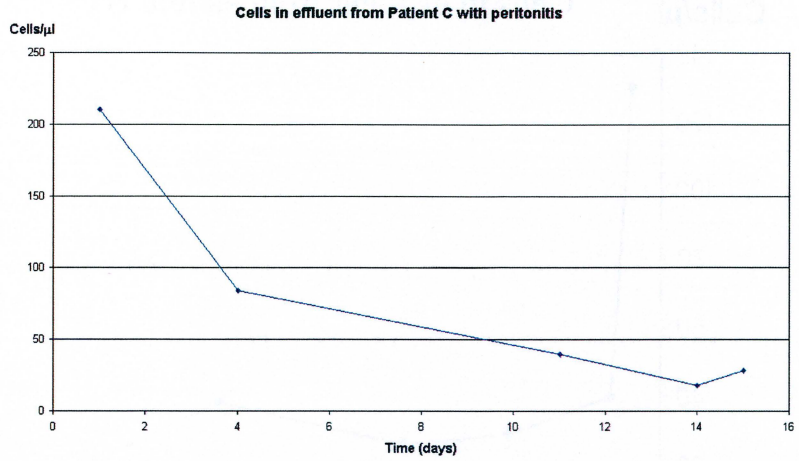

Figure 43. Cell concentration in the effluent from Patient C recovering from peritonitis. The cell concentration was measured with the Bürker chamber.

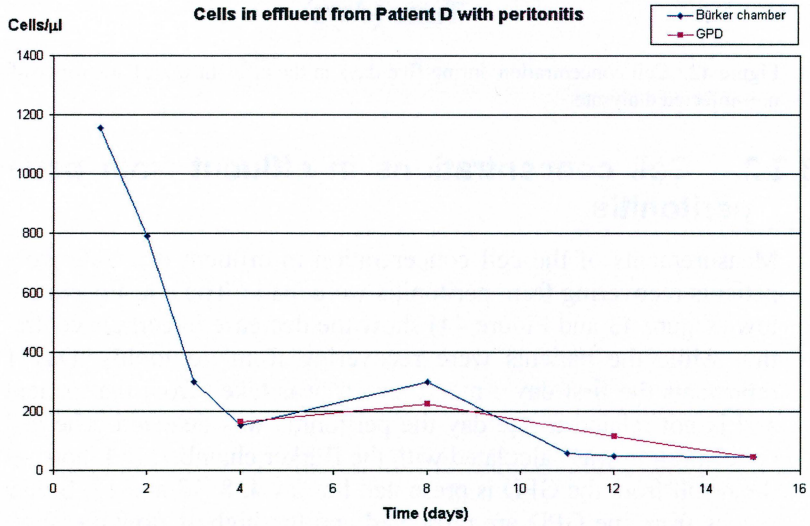

Figure 44. Cell concentration in the effluent from Patient D recovering from peritonitis. The cell concentration was measured with the Bürker chamber. In the same figure the GPD results can be found for day 4, 8, 12 and 15.

Day	Cell concentration (cells/ml)	GPD result (cells/µl)	Flow (ml/min)
4	152	163	80
8	300	224	220
12	48	116	96
15	44	46	80

Table 1. Cell concentration according to the NucleoCounter for Patient D, cell concentration according to the GPD and the flow used in the measurement plotted in Figure 44.

3.3. Two-dimensional scattering measurements

The analysis of the pictures as described in the methods section on page 20 is summarized in Figure 45. The results from two-dimensional scattering measurements on 45- and 20 cells/µl are presented in Figure 46 and Figure 47.

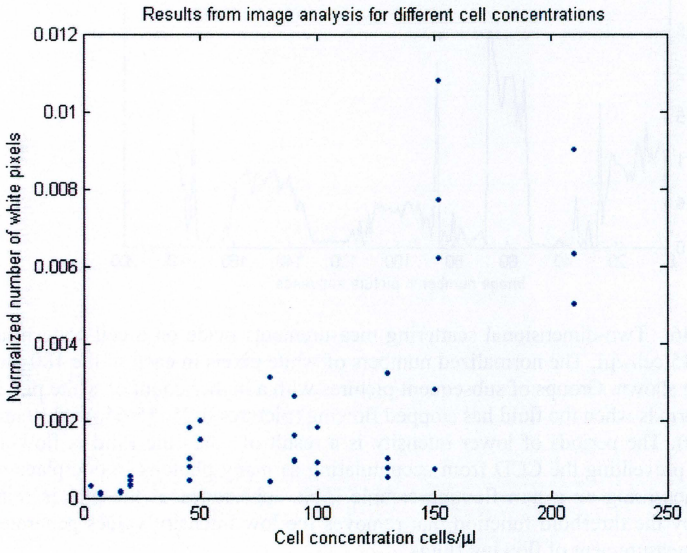

Figure 45. Normalized counts of filtered pixels registered above threshold with the two-dimensional detector versus different cell concentrations. Every dot represents the mean signal taken from a single sample volume.

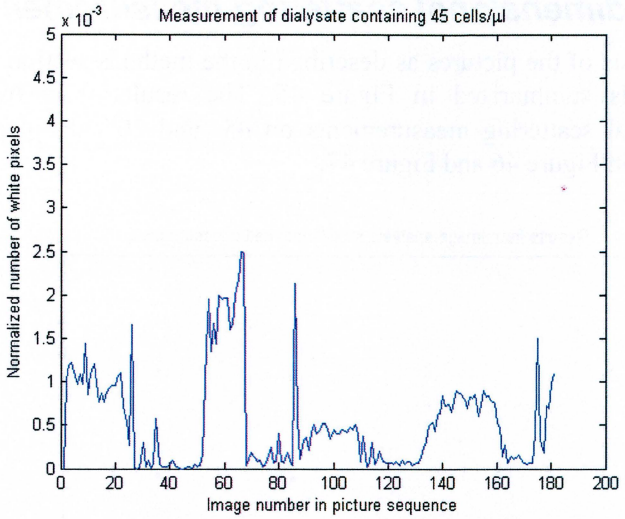

Figure 46. Two-dimensional scattering measurements made on a cell concentration of 45 cells/µl. The normalized numbers of white pixels in each of the 180 pictures are shown. Groups of subsequent pictures with a higher count of white pixels show periods when the fluid has stopped flowing (pictures 0-25, 55-65, 85-110 and 135-160). The periods of lower intensity is a result of when the fluid is flowing thereby preventing the CCD from accumulating as many photons in one place as when measuring on a non flowing sample. This appearance of the plot is reinforced by the threshold function that removes the low intensity values generated during measurement of flowing fluids.

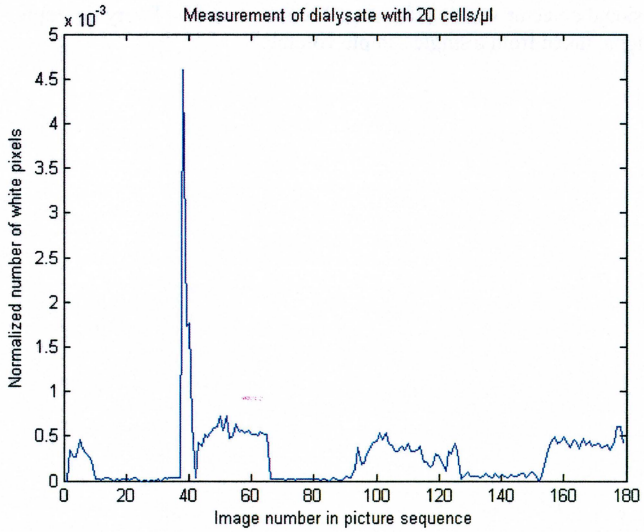

Figure 47. Two-dimensional scattering measurements made on a cell concentration of 20 cells/µl. The normalized numbers of white pixels in each of the 180 pictures are shown. Groups of subsequent pictures with a higher count of white pixels show periods when the fluid has stopped flowing (pictures 0-10, 38-65, 90-125 and 155-180). The periods of lower intensity is a result of when the fluid is flowing thereby preventing the CCD from accumulating as many photons in one place as when measuring on a non flowing sample. This appearance of the plot is reinforced by the threshold function that removes the low intensity values generated during measurement of flowing fluids. The high peak centered around picture number 40 is caused by a air bubble causing a strong signal in the CCD.

3.4. Absorption measurements

The absorption measurement shows that the PVC-material of the tube has a high absorption of wavelengths shorter than approximately 380 nm. In the rest of the visible range the absorption is low.

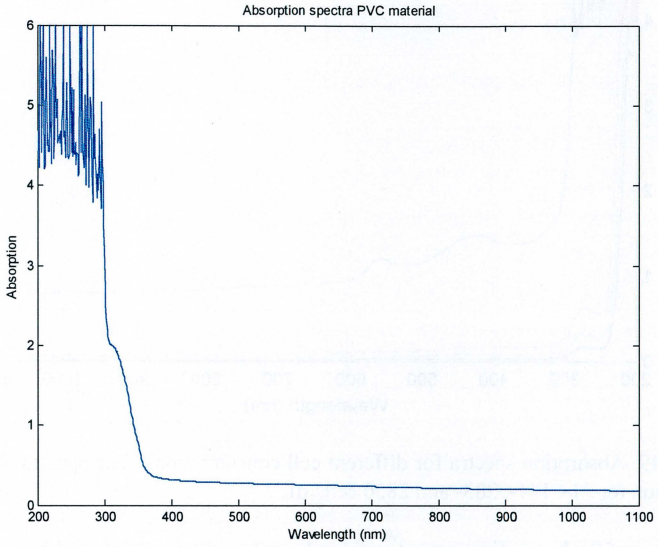

Figure 48. Absorption spectrum of the PVC-material used in the tube. The PVC-material absorbs wavelengths below approximately 370 nm.

As can be seen in Figure 48 there is no use in looking for absorption peaks in wavelengths below 370 nm as all light is fully absorbed by the PVC tube.

As an increased amount of cells in the patient dialysate is a key factor in detection of peritonitis, absorption spectra for different cell concentrations of the L929 cells were studied. The results can be seen in Figure 49.

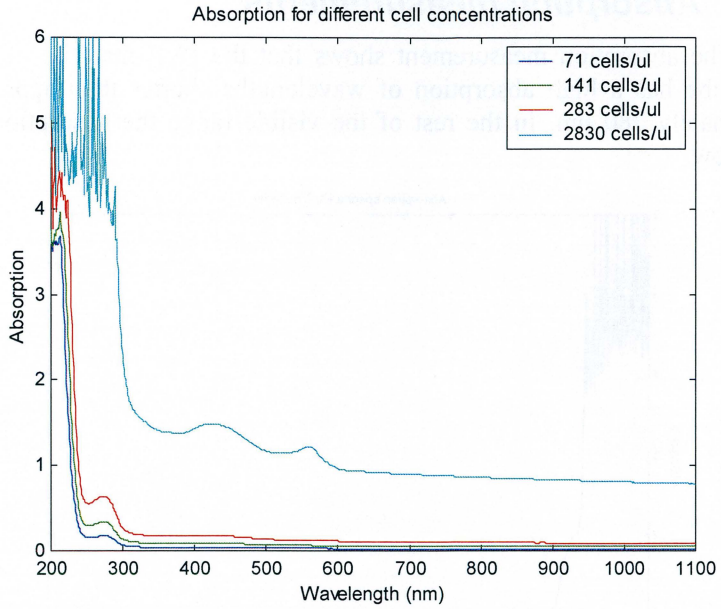

Figure 49. Absorption spectra for different cell concentrations. The spectra shows absorption for 71-, 141-, 283- and 2830 cells/µl.

In Figure 50 absorption spectra for phenol red are shown. The spectra was taken as the cells measured in
Figure 49 are diluted in a solution containing phenol red (see discussion).

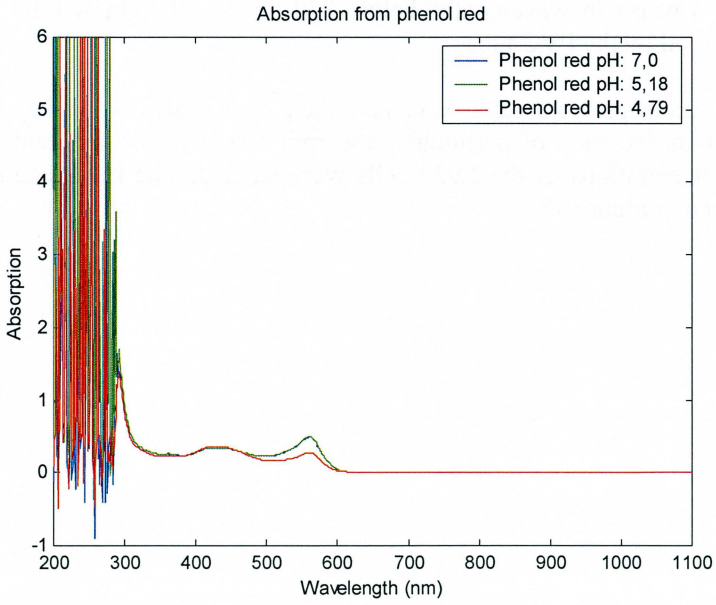

Figure 50. Absorption spectra for phenol red. The phenol red was diluted in suspensions with the pH values 7.0, 5.18 and 4.79.

Patient effluent also contains albumin and other proteins. Figure 51 shows the absorption spectra for 1, 4 and 40 M albumin.

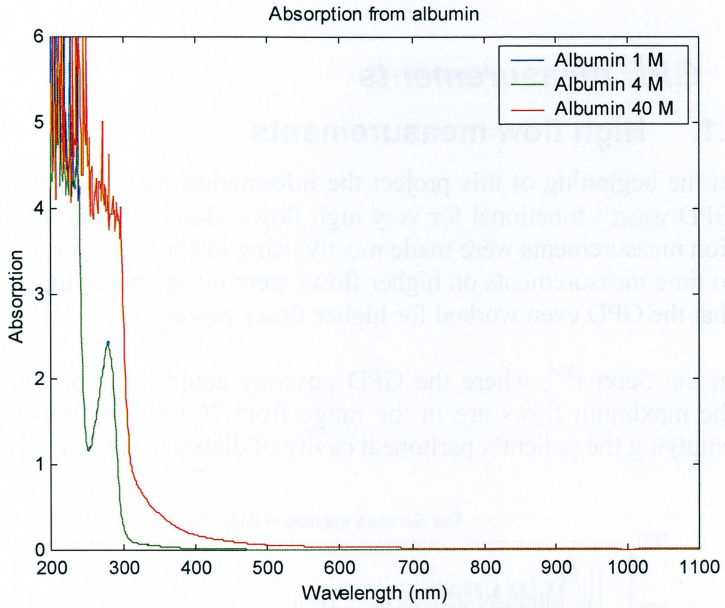

Figure 51. Absorption spectra for albumin with the following concentrations 1-, 4- and 40 M. The absorption curve for 1 M is hidden behind the absorption curve for 4 M.

4. Discussion

4.1. GPD measurements

4.1.1. High flow measurements

In the beginning of this project the information was given that the GPD wasn't functional for very high flows. Based on this information measurements were made mostly using lower flows. From time to time measurements on higher flows were made and an indication that the GPD even worked for higher flows was seen.

In the Serena™, where the GPD possibly could be implemented, the maximum flows are in the range from 200-500 ml/min while emptying the patient's peritoneal cavity of dialysate (Figure 52).

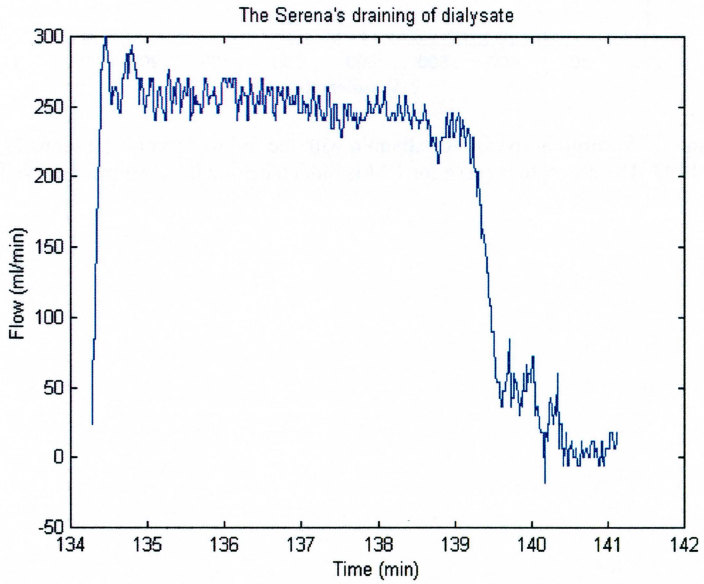

Figure 52. Flow during the draining of dialsysate from a patient using the Serena™.

At this emptying phase the flow remained quite stable during several minutes and it would be ideal for a measurement. Using lower flows would require a control of the flow with help from the Serena™, but high flow measurements would only require the flow as an input parameter. This parameter is already monitored in the Serena™ and would be available for the GPD to use.

The standard deviation for the GPD using the GPD algorithm didn't differ considerably from the standard deviation for the NucleoCounter™ which is a recognized tool for determination of cell concentrations. The NucleoCounter™ stained the cells nucleus with a

dye that fluoresced when activated with ultra violet light. This discriminated between particles and cells. No such discrimination was done using the GPD as it counted every particle that scattered the laser light.

4.1.2. Low flow measurements

Using low flows could often show a wide spread in results when using the GPD algorithm. This was why a more stable algorithm was sought. The peak counting algorithm showed promising results for low flows compared to the GPD algorithm (see Figure 30), but had the disadvantage of not being functional for higher cell concentrations.

In Figure 29 in the result section, an indication can be seen that a measurement using a high flow gives a better accordance to the actual cell concentration than a measurement using a low flow.

4.1.3. Flow dependence in the GPD algorithm

A very clear dependence between the chk_point variable and the flow is seen in Figure 40 shown in the results section. As can be seen in the figures, the errors to the regression curves in a least square sense, becomes smaller as the flow and cell concentration increases. This motivates measurements at higher flows. A possible explanation to the non-linear conditions seen in flow dependence is given in the discussion section for high flow measurements. The chk_point variable is extracted from the histogram containing the segmented signal strengths. When measuring on low flows there is a larger variation of signal strengths because the photodiode in the GPD generates larger and more defined voltage peaks for low concentrations and flows. At higher flows and cell concentrations the overall signal strength rises and gets more evenly distributed in the histogram. This could also be a reason why there is a more stable correlation between the flow and the chk_point variable at higher flows and cell concentrations.

4.1.4. The peak counting algorithm

4.1.4.1. Data acquisition and analysis

The most direct way of measuring the amount of cells in a solution with the current setup was to count each individual peak in the signal. This sets high demands on the sampling frequency of the system. A rough approximation of the number of cells passing through the laser beam was made (see Figure 53). The approximation took into account the size of the laser beam inside the tube, the dimensions of the tube, the flow and the cell concentration of the solution. It was also assumed that the particles were suspended homogenously in the solution.

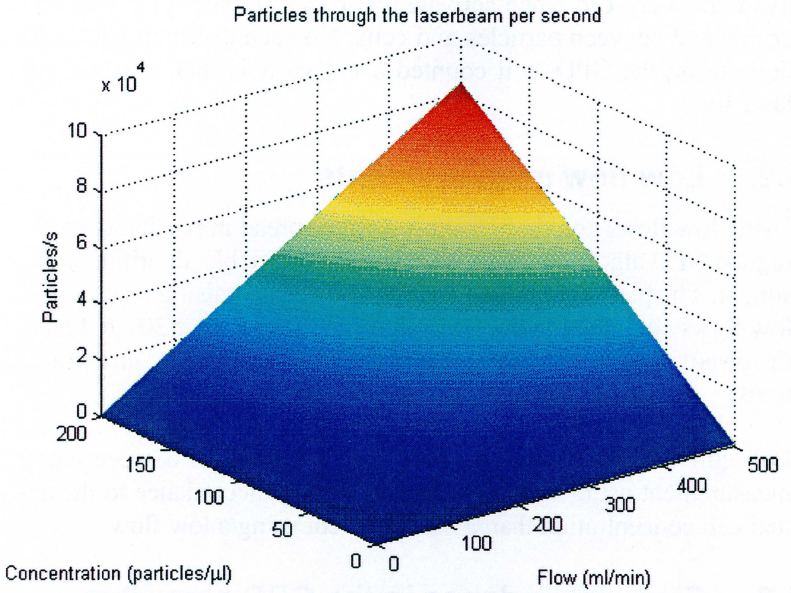

Figure 53. Theoretical calculation of the number of particles that would flow through the laserbeam per second in the GPD. This calculation was based on the assuption of a homogenous suspension of particles.

The photodiode S8745-01 had a sampling frequency of about 25 Hz in its default setting. That meant that the amplification was relatively large and the peaks were well defined. By reducing the amplification the frequency could be increased but the peaks in the signal lost a significant amount of contrast towards the background noise. The peak counting algorithm showed inconsistent values for higher cell concentrations. For higher concentrations and flows the peak counting algorithm didn't create a linear relationship between the signal generated by the GPD and the cell concentration. For low flows and concentrations the signal was weak due to small amounts of scattering particles but peaks were easy to distinguish. For higher flows and cell concentrations the signal generated by the GPD changed. Peaks were no longer easily discriminated with one uniform threshold for the entire sample period. Several peaks were packed in bundles at different signal strengths making the threshold used in the peak counting algorithm useless. Either way the uniform threshold was placed meant that the peak counting algorithm counted too few peaks. This was the reason that the peak counting algorithm didn't manage to give consistent values for solutions containing higher cell concentrations. The peak counting algorithm always gave lower values than the actual cell concentration for high flows and high cell concentrations.

From Figure 34 it is clear that the data modified by the sliding mean makes it easier to discriminate between what should be one peak and what should be several peaks. This was useful when measuring on low signal strengths and cell concentrations which was the case for the peak counting algorithm.

The peak counting algorithm works well for cell concentrations up to approximately 25 cells/µl and flows up to 80 ml/min. This may seem strange as a cell concentration of 10 cells/µl and a flow of 20 ml/min will have the same amount of cells passing through a cross section of the tube as a cell concentration of 20 cells/µl and a flow of 10 ml/min.

An explanation to this and the non-linear flow dependence in the GPD algorithm and peak counting algorithm could be the "tubular pinch effect". Experiments have shown that particles tend to move to a certain equilibrium position in the tube at about 0.6R, where R is the tube radius (see Figure 54). These experiments were done on neutrally buoyant solid spherical particles in laminar flow [18]. The migration of the particles occurs both for particles originally placed in the center (migrating outwards) of the tube and for particles near the tube wall (migrating inwards) [22]. With an increased flow there will be an accumulation of particles at 0.6R. This may explain why the amount of peaks in the GPD-signal is not proportional to the flow.

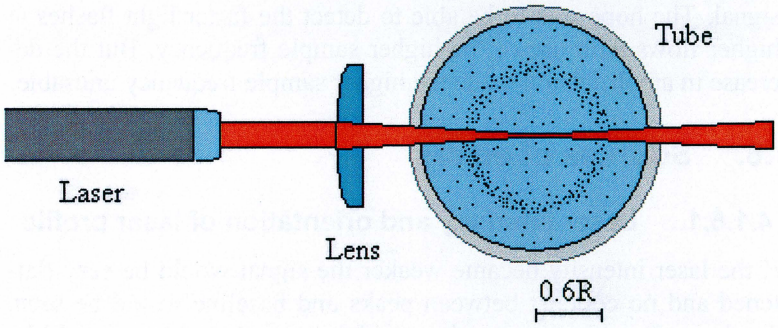

Figure 54. The "tubular pinch effect". Particles in flow tend to move to a certain equilibrium position in the tube at about 0.6R, where R is the tube radius. The figure shows a cross section of the tube and the expected accumulation of particles at 0.6R.

In Figure 38 to Figure 39 the influence of an increase in flow and cell concentration is compared respectively. An important factor to know is if the signal changes linearly independent of which of these parameters that are changed. An increase in the cell concentration gives rise to a lot more peaks that an increase in the flow. For lower cell concentrations there are a clear contrast between a baseline and a peak but as the concentration increases this contrast gets less clear. As can be seen in Figure 39 peaks start to merge together and are hard to distinguish.

The peak counting algorithm has the advantage of making accurate estimations for low cell concentration. However, the range in terms of flows and cell concentrations in which the peak counting algorithm functions is insufficient for the purpose at hand. The peak

counting algorithm was accurate for flows below 80 ml/min and cell concentrations below 25 cells/µl. When it's needed to accurately see the change in cell concentrations above 25 cells/µl the peak counting algorithm can no longer be used. Even though the problem with measuring higher cell concentration could be overcome it has another flaw in not being able to track cell concentrations at higher flows. To be implemented with the Serena™ it would be preferable for it to be able to handle flows around 200-500 ml/min. These requirements and the lack of accurate results gained from the peak counting algorithm at higher flows and cell concentrations put a halt to further use of this algorithm. The good results acquired by the GPD algorithm at high flows stopped the need for further developing the peak counting algorithm.

4.1.5. Attempts to increase the sample frequency of the detector

After measurements with different sample frequencies the conclusion was reached that the original sample frequency (without any external feedback resistors connected) was the most appropriate to use. What was gained in frequency, was lost in amplification of the signal. The hope was to be able to detect the faster light flashes at higher flows with use of the higher sample frequency. But the decrease in amplification made the higher sample frequency unusable.

4.1.6. Sources of errors

4.1.6.1. Laser intensity and orientation of laser profile

If the laser intensity became weaker the signal would be very flattened and no contrast between peaks and baseline would be seen. To determine this a comparison with a new unused laser could be done, as it could be difficult to see if a small laser spot had become weaker or not.

The light profile of the laser used was oval shaped and the orientation of the profile affects the results in a way that was not expected. If the profile was orientated vertically it seemed like cells were passing through a so narrow focal point that flashes of light were merely detectable.

If the laser profile was orientated horizontally the cells seemed to pass through a larger lit area and the peaks arising from cells were very broadened and not well defined.

What was found to be the optimal orientation of the oval laser profile was a 10 to 15° rotation from the vertical position. The dramatic change in the signal's appearance is shown in Figure 36. All plots are showing a 2 second measurement on the same dialysate containing a cell concentration of 152 cells/µl.

4.1.6.2. Errors in calculation of cell concentration

There were problems with getting samples to have the designated cell concentrations. The samples were produced by diluting a known concentration into several samples of lower concentrations. The reasonably large uncertainty in such samples was first discovered when it was decided to make a verification measurement on the diluted samples with the NucleoCounter™ after a puzzling result during a measurement. This showed that measurements made without making a verification of the cell concentration on each diluted sample wasn't as reliant as expected. This may explain some inconsistency in the results from measurements made without verification of each sample.

As was mentioned above, the cell concentration calculated by dilution wasn't always the cell concentration that one ended up with. A recommendation is to always confirm the cell concentration with some other reliable method. This was especially important if the cell solution measured on would be used for calibration of an algorithm or similar.

4.1.6.3. Aggregation and precipitation in dialysate

What was found to be a source of error was that effluent dialysate contains microorganisms that can increase in amount with time. This process is more rapid if the dialysate is not kept cold. That meant that when the GPD measured on the same sample at a later time the result would differ substantially from the first measurement. Measuring on the dialysate at a later time always gave a higher result than the first measurement. This should not be considered a problem when implementing the GPD because the idea is to measure on the dialysate at the actual draining of the patient and not as in the case of the experiments, as much as one or a couple of days later. The NucleoCounter™ still showed the same cell concentration after measuring on the same sample a second time. The GPD produced a higher result for the second time.

Bags containing dialysate that hade been kept outside the refrigerator could show visible pieces of aggregated and precipitated material. The dialysate could also have a more cloudy appearance. When measured on with the detector (that detects all scattering material) one could see a saturation of the photo detector (reaching the maximal signal level of 5 in the workspace). This would normally imply an extremely high cell concentration.

4.1.6.4. Blood present in the dialysate

One of the bags received from a patient contained blood. As the laser used has a wavelength of 630 nm (red light) the scattering from the red blood cells will be very prominent. The presence of blood in the effluent dialysate is not considered normal or healthy. Any false

alarm in the GPD caused by red blood cells should be accepted as it is a symptom that would warrant a medical examination.

4.1.7. Limitations

- The GPD is dependent of the flow as an input parameter.
- The GPD has no ability to distinguish between cells and other light scattering material.
- Drain bag tubes can have different optical properties that could affect the GPD's result.
- Dirt on the drain bag tube can block the laser from passing through the tube.

4.2. Patient studies

It came as a surprise to see such a high cell concentration as 130 cells/µl for Patient B (Figure 42). One plausible explanation was that the patient had fallen ill in pneumonia and started treatment on antibiotics. The decrease in cell concentration that can be seen from day one to day two could probably be the antibiotics taking effect. An explanation to why there was an increase in cell counts for Patient A day 4 could not be found. Strangely enough an increase at this same day and time interval could also be seen for Patient B. A possible explanation could be the human error as three different people took turns on calculating the cell concentration with the Bürker chamber. Considering that this study only followed two patients under a small period of time the results can't be seen as representative for the general PD patient group. One of the patients was also recovering from pneumonia which very likely seemed to have affected the measurements.

4.3. Two-dimensional scattering measurements

The two-dimensional setup was crude and mechanically instable. It proved difficult to find the right plane of focus when the slightest movement could put the camera out of focus. It was also difficult to determine which part inside the tube to focus on. When examining the original pictures there are several bright spots aside from the ones generated by particles in the solution. These spots could come from different refraction phenomenon in the tube. There was also the possibility that there were cells or particles that had attached themselves to the inner wall of the tube. These spots arising from static light scattering could easily be discarded from with a background subtraction.

By tuning the focus of the macro objective different planes of the tube came in focus. This could give a different amount illuminated cells depending on the plane of focus. The result shown in Figure

45 shows a vague correlation between an increase in cell concentration and the normalized count of bright pixels above a certain threshold value. There were a number of factors contributing to this poor correlation, but none of them should be too difficult to overcome. Air bubbles proved to be a problem in this first pilot study with this method as there wasn't time enough to develop and take into advantage the image analysis techniques that could be used to reduce the disturbing signals arising from air bubbles.

In future analysis and refinement of an algorithm one could use different image analysis techniques to filter disturbing objects in the picture. One reason for the wide spread in results could be the small sample volume taken for each clamp and measure procedure. The amount of 4.5 µl per sample may not be entirely representative for the entire volume of approximately 2 liters. This could be compensated for with an increased number of more effective and automated clamp and measure runs. The problems with inconsistency between different clamp and measure runs on the same cell concentration can be seen in Figure 46. This can be compared with a more consistent sequence of measurements shown in Figure 47.

With sufficient magnification this technique of two-dimensional measurements could open up a new possibility of automated analysis of cells in peritoneal dialysate effluent. The testing of this method was mostly limited by the limited time that the instrument could be borrowed, time available to thoroughly build a stable setup and the lack of compatible optics. Even though the setup was created for measuring on non flowing solutions the use of a two-dimensional detector gives the opportunity to track the speed of particles by means of vision based particle tracking [23]. This could exclude the need for an extra sensor to determine the flow when measuring on flowing solutions.

To make such an instrument cost efficient there would have to be further investigation on what type of specifications needed from both CCD-chip and optics. The camera and macro objective borrowed from Hamamatsu together would cost approximately 8000 €. This is a considerable amount but the camera used had higher standards than needed for such an application.

4.4. Absorption

From the absorption measurements it was evident that the wavelengths used in analysis of the tube's contents had to be within the visible range. The idea of using absorbance analysis was inhibited by the high absorbance of shorter wavelengths in the PVC-material.

In the absorption measurements of different cell concentrations there were two peaks at wavelengths 420 nm and 570 nm (see Figure 49). These peaks are a result of the phenol red substance that is a pH indicator (see Figure 50). This pH indicator was used to

survey the cells, as they were cultivated in the lab. The increase of these peaks with higher cell concentration was consistent with the increased amount of phenol red.

There were an overall increase of absorption in the spectrum with increasing cell concentrations but the difference was relatively small and hard to discriminate between at low cell counts. Albumin showed no absorption peaks outside the range that would be absorbed by the PVC tube. From this, the conclusion was drawn that absorption measurements on dialysate wasn't a useful method for detection of peritonitis.

5. Conclusion

The potential of the GPD to make an early detection of peritonitis with a relatively simple and cheap setup deserves further attention. Results from experiments conducted in this diploma work indicates that the GPD and GPD algorithm could be implemented with the APD-machine Serena™ without making any changes to tube sets or flow parameters. The other available methods such as the Serim™ Periscreen™ strips or more elaborate laboratory methods such as the Bürker chamber or the NucleoCounter™ all demand that samples are taken from the dialysate or at least some kind of direct contact with the effluent dialysate.

The GPD would have low running costs, give easy readings and continuously provide important information about the patient. The first step would be to implement the GPD with the APD machine Serena™. It should easily fit the existing schedule of annual service made on those machines. To make daily analysis of effluent dialysate with test strips don't only involve extra work and more contact with effluent but would also generate a cost of approximately 900 € per year. This is a cost that probably would exceed the cost of the GPD when it is implemented. This calculation is based on that the strips are used once per day compared to the GPD that can be used many times per day.

The flows that were used when draining the peritoneal cavity from dialysate seem to be suitable for measurements with the GPD. At these flows the results shows good accordance with the results from recognized devices like the NucleoCounter™. Even for use without the Serena™ there could be a possibility to use the GPD in CAPD.

A further study of what cell concentrations can be considered normal in dialysate is needed. The study of the two patients in this diploma work was not sufficient. Will there be a high variability from patient to patient? If so, will there be a need to adjust the GPD's algorithm for every patient? In either way the GPD shows promising results to be able to follow an ongoing increase in cell concentration. This will hopefully detect peritonitis at a much earlier stage than is done today and prolong the technique survival with peritoneal dialysis.

6. Future improvements

Even though the GPD shows great promise it needs further improvements before being implemented for patient use.

- **Investigate which type of laser to be used**
  The laser used in this project was a cheap class 1 laser. Before implementing the GPD for patient use the specifications of the laser should be well defined especially concerning life time, intensity and appearance of the laser spot since these parameters seemed to affect the result of the GPD drastically.

- **Implement laser intensity check**
  The laser intensity reduced drastically during some of the experiments due to overload of the laser. This generated an answer with lower cell concentrations than actually measured on. To avoid this problem a calibration system or a sensor determining the laser intensity before each measurement could be implemented.

- **Make the GPD user friendly**
  The GPD prototype is instable and demands a bit of experience of the user for it to produce adequate signals. The procedure developed during this diploma work for checking that the GPD worked properly before each experiment was time consuming and complicated. To avoid this procedure new mounts and holders has to be built. The laser, photodiode and lenses have to be firmly secured to avoid that any of the components are moved between or during measurements.

- **Test the GPD with patients**
  Even though there are strong indications that the GPD may function there are no encompassing tests of it made with larger groups of patients. All the experiments done in this diploma work were made at the lab some time after the actual draining of the patient. Can the appearance of the dialysate differ at the actual draining? Is there need for modification in the algorithm or setup for each patient? How does the WBC concentration change at the start of an episode of peritonitis? How common is it for patients to have higher concentrations of other particles than WBC, which affect the GPD signal, in their dialysate? Answers to these questions should be investigated.

7. Acknowledgements

We wish to express our gratitude to ...

Ola Carlsson, Gambro, for his invaluable help and supervision of this diploma work.

Jenny Svensson, Division of Atomic Physics at Lund Institute of Technology, for her guidance, help and supervision.

Per Kjellstrand, Gambro, for continuously giving feedback on our work.

Anders Wieslander, Gambro, for his encouragement and feedback during the diploma work.

Per Hansson, Gambro, for his help with electronics and to facilitate flow measurements.

Olof Jansson, Gambro Treatment System Research, for his support and feedback on algorithm development.

Tobjörn Linden, Gambro, for the help with electronics.

Eva Svensson, Gambro, for providing us with L929 cells from the cell laboratory at Gambro.

Karin Stagne, for help with transport of patient dialysate.

Eddie Nilsson, Gambro, for the help with construction of experimental equipment.

Prof. **Anders Axelsson**, at the Centre for Chemistry and Chemical Engineering at Lund Institute of Technology, and **Mariagrazia Marucci**, LTH, for their help on theory about behavior of particles in flow.

Prof. **Björn Holmquist**, Department of Mathematical Statistics at Lund Institute of Technology, for his advice on mathematical problems that was encountered during the diploma work.

Ann-Britt Grahed at the PD clinic at MAS for suppling us with patient dialysate.

The staff at **Arendala** nursing home and **Annegårds** nursing home in Lund for providing us with patient dialysate.

Martin Erixon, Behnaz Mostafavi, Charlotte Berg, Josefin Ahlberg, Petronella Schröder, Helena Jepsson, Christian Olsson, Johanna Dennbo, Evi Martinson, Agnes Lukacs, Lena Olsson, Carin Bergsten and Fabienne Olsson for help with various tasks and nice lunches.

To all other **people working at Gambro** for all our nice chats and for making us feel welcome.

8. References

1. L. Gotloib, A. Shostak and V. Wajsbrot, *Functiontional structureof the peritoneum as a dialysis membrane,* in Textbook of Peritoneal Dialysis 2 ed. Edited by Gokal R, Krediet R and Nolph K 2000:Kluwer Academic Publishers, p. 37-106. ISBN 0-7923-5967-4

2. The Cleveland Clinic homepage. http://www.clevelandclinic.org/nephrology/patient/dialysis.htm (Visited 2006-05-11)

3. Gambro homepage. http://www.gambro.com/Pages/InfoPage.aspx?id=479 (Visited 2006-05-25)

4. Journal of the American Society of Nephrology homepage. http://jasn.asnjournals.org/cgi/content/full/13/suppl_1/S104#R6-099277 (Visited 2006-05-23)

5. David J. Leehey, Vasant C. Gandhi and John T Daugirdas, *Peritonitis and Exit Site Infection,* in Handbook of Dialysis Third Edition. Edited by John T. Daugirdas, Peter G. Blake and Todd S. Ing 2001: Lippincott Williams & Wilkins, p. 373-398.

6. L. Fried and B. Piraino, *Peritonitis,* in Textbook of Peritoneal Dialysis 2 ed. Edited by Gokal R, Krediet R and Nolph K 2000:Kluwer Academic Publishers, p. 545-564. ISBN 0-7923-5967-4

7. Gambro Basic. Study material over the basic principles of dialysis. (2004)

8. Gry E. Albrektsen, MD, Tor-Erik Widerøe, MD, PhD, Tom I.L. Nilsen, PhD, Pål Romundstad, PhD, Maria Radtke, MD, Stein Hallan, MD, PhD, Knut Aasarød, MD, PhD, Cecilia Øien, MD, and Inger K. Lægreid, MD, " Transperitoneal water transport before, during, and after episodes with infectious peritonitis in patients treated with CAPD", American journal of Kidney Diseases, vol 43, No 3 (March), pp 485-491 (2004).

9. Seong-Joo Park, Joon-Yeop Lee, Woo-Taek Tak, Jeong-Ho Lee. *Using reagent strips for rapid diagnosis of peritonitis in peritoneal dialysis patients.* Advances in Peritoneal Dialysis, 2005, Vol. 21.

10. Serim research corp. homepage. http://www.serim.com/products_dialysis_periscreen.htm (Visited 2006-05-10)

11. R. Domann, Y. Hardalupas and A R Jones, "A study of the influence of absorption on the spatial distribution of fluorescence intensity using Mie theory, geometrical optics and imaging experiments", Meas. Sci. Technol. **13** (2002) 280-291.

12. V. J. Morris and B. R. Jennings, "Light scattering by bacteria I. angular dependence of the scattered intensity", Proc. R. Soc. Lond. A. **338**, 197-208 (1974).

13. Alexander A Kokhanovsky, "Optical properties of bubbles", J. Opt. A.: pure Appl. Opt. **5** 47-52 (2003)

14. S. P. Srinivas, Joseph A. Bonanno, Els Larivière, Danny Jans and Willy Van Driessche, "Measurment of rapid changes in cell volume by forward light scattering", Eur J Physiol 447:97-108 (2003).

15. Ye Yang, Zhen-Xi Zhang, Xin-Hui Yang and Da-Zong Jiang, "The blood cell counting and classification from stationary suspensions by laser light scattering method", Proceedings of IEEE engineering in Medicine and Biology Society, Vol. 20, No 4, (1998).

16. Masayuki Niwa, Yutaka Kanamori, Ken-Ichi Kohno, Hiroyuki Matsuno, Osamu Kozawa, Mitsutaka Kanamaru and Toshihiko Uematsu, "Usefulness of grading of neutrophil aggregate size by laser-light scattering technique for characterizing stimulatory and inhibitory effects of agents on aggregation", Life sciences **67**, 1525-1534 (2000).

17. Joris R. Delanghe, Timo T. Kouri, Andreas R. Huber, Kurt Hannemann-Pohl, Walter G. Guder, Andreas Lun, Pranav Sinha, Gudrun Stamminger and Lothar Beier, "The role of automated urine particle flow cytometry in clinical practice", Clinica Chimica Acta **301**, 1-18 (2000).

18. Erling, Eklund. A study of Particle-Fluid Phenomena in Bounded Shear Flows Numerical simulation and experimental modelling, Licenciate dissertion October 1990.

19. Hamamatsu homepage. http://sales.hamamatsu.com/en/products/solid-state-division/si-photodiode-series/with-preamp-cooler/s8745-01.php?&group=1 (Visited 2006-03-07)

20. Hamamatsu homepage. http://sales.hamamatsu.com/en/products/system-division/cameras/uv-vis-ir/c8484-05.php (Visited 2006-05-17)

21. Sarah S. Prichard, *Metabolic Complications of Peritoneal Dialysis* , in Handbook of Dialysis Third Edition. Edited by John T. Daugirdas, Peter G. Blake and Todd S. Ing 2001: Lippincott Williams & Wilkins, p. 407-408.

22. Nano Medicine Book Site homepage. http://www.nanomedicine.com/NMI/9.4.1.4.htm (Visited 2006-05-22)

23. A. Baldassarre, m. De Lucia, P. Nesi and F.Rossi, "A vi-son-based particle tracking velocimetry", Real time imag-ing **7**, 145-148 (2001).

24. Plastics USA homepage. http://www.plasticsusa.com/pvc.html (visited 2006-05-11)

25. New Brunswick Scientific Co. homepage. http://www.nbsc.com/products/cellcounters/NucleoCounter.asp (Visited 2006-04-28)

26. Health protection Agency homepage. http://www.hpa.org.uk/radiation/faq/laser/laser9.htm (Visisted 2006-05-23)

9. Appendix

9.1. The NucleoCounter™

The NucleCounter™ is a device developed by New Brunswick Scientific Co., Inc [25]. It is recognized as an accurate cell counter and is widely used for determination of cell concentrations. Comparisons to this device will be made through out this report.

The NucleoCounter system consists of:

- A NucleoCounter with highly-advanced fluorescence microscope, charged-coupled device (CCD) camera, and hardware-based image analysis (Figure 55).
- Disposable NucleoCassettes with piston **(A)** to aspirate a pre-defined volume of your sample into the cassette; **(B)** nuclei-staining dye; and **(C)** window where sample will be read by the NucleoCounter (Figure 56).
- Reagents for cell lysis and stabilization.
- Optional NucleoView™ PC software for documentation, image viewing and data processing.

Figure 55. The NucleoCounter™.

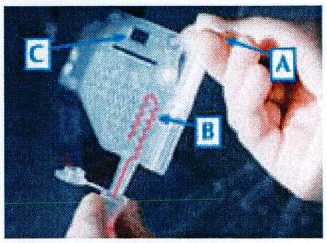

Figure 56. The NucleoCassette™.

9.2. The Bürker chamber

The Bürker chamber is used to count cells, spors and particles in a well defined volume with high accuracy using a microscope.

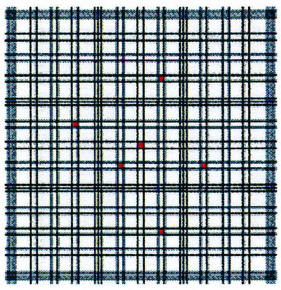

a.

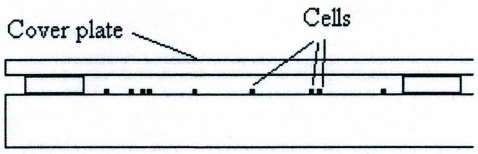

b.

Figure 57. a. The Bürker chamber. b. Side view of the Bürkerchamber showing the cover plate and cells.

9.3. Class 1 laser

Class 1 lasers are products where the irradiance (measured in watts per metre square) of the accessible laser beam (the accessible emission) does not exceed the Maximum Permissible Exposure (MPE) value. Therefore, for Class 1 laser products the output power is below the level at which it is believed eye damage will occur. Exposure to the beam of a Class 1 laser will not result in eye injury and may therefore be considered safe. However, some Class 1 laser products may contain laser systems of a higher Class but there are adequate engineering control measures to ensure that access to the beam is not reasonably likely. Examples of such products include laser printers and compact disc players. Anyone who dismantles a Class 1 laser product that contains a higher Class laser system is potentially at risk of exposure to a hazardous laser beam [26].